LBNL-43906
Preprint

ERNEST ORLANDO LAWRENCE
BERKELEY NATIONAL LABORATORY

# Equation of State for Thermodynamic Properties of Chain Fluids Near-to and Far-From the Vapor-Liquid Critical Region

Jianwen Jiang and John M. Prausnitz
**Chemical Sciences Division**

July 1999
Submitted to
*Journal of Chemical Physics*

REFERENCE COPY
Does Not
Circulate
Bldg. 50 Library - Ref.
Lawrence Berkeley National Laboratory
Copy 1
LBNL-43906

## DISCLAIMER

This document was prepared as an account of work sponsored by the United States Government. While this document is believed to contain correct information, neither the United States Government nor any agency thereof, nor the Regents of the University of California, nor any of their employees, makes any warranty, express or implied, or assumes any legal responsibility for the accuracy, completeness, or usefulness of any information, apparatus, product, or process disclosed, or represents that its use would not infringe privately owned rights. Reference herein to any specific commercial product, process, or service by its trade name, trademark, manufacturer, or otherwise, does not necessarily constitute or imply its endorsement, recommendation, or favoring by the United States Government or any agency thereof, or the Regents of the University of California. The views and opinions of authors expressed herein do not necessarily state or reflect those of the United States Government or any agency thereof or the Regents of the University of California.

LBNL-43906

# Equation of state for thermodynamic properties of chain fluids near-to and far-from the vapor-liquid critical region

Jianwen Jiang and John M. Prausnitz
Department of Chemical Engineering
University of California
and
Chemical Sciences Division
Lawrence Berkeley National Laboratory
University of California
Berkeley, CA 94720, U.S.A.

July 1999

This work was supported by the Director, Office of Science, Office of Basic Energy Sciences Chemical Sciences Division of the U.S. Department of Energy under Contract Number DE-AC03-76SF00098.

# Equation of state for thermodynamic properties of chain fluids near-to and far-from the vapor-liquid critical region

**Jianwen Jiang and John M. Prausnitz** [a)]

*Department of Chemical Engineering, University of California, Berkeley and Chemical Sciences Division, Lawrence Berkeley National Laboratory, University of California, Berkeley, California 94720*

Upon incorporation of contributions from long-wavelength density fluctuations by a renormalization-group theory, a crossover equation of state is developed for describing thermodynamic properties of chain fluids. Outside the critical region, the crossover equation of state reduces to the classical equation; inside the critical region, it gives non-classical universal critical exponents. The crossover equation of state correctly represents phase equilibria and $pVT$ properties of chain fluids in both regions. Good agreement is obtained upon comparisons with computer simulations for square-well chain fluids. As obtained from experimental vapor-pressure and density data, the square-well segment-segment parameters for $n$-alkanes from ethane to eicosane are linear functions of molecular weight. Calculated thermodynamic properties agree well with experiment for $n$-alkanes from methane to hexatriacontane.

[a)] To whom correspondence should be addressed. Electronic mail: lindar@cchem.berkeley.edu

## I. INTRODUCTION

Thermodynamic properties of fluids at high pressures are of much interest in a variety of chemical industrial processes, notably for separation processes in natural-gas and gas-condensates production, for supercritical extraction, and for fractionation of petroleum.[1,2] Some of these separation processes encounter critical conditions.

Following the van der Waals equation of state (EOS)[3], dozens of similar phenomenological EOS have been proposed; those by Redlich and Kwong[4] and by Peng and Robinson[5] are the best known. These equations can describe fluid properties reasonably well far away from the critical point; however, it has been long recognized that, because they are based on the mean-field assumption, they do not yield the correct limiting properties at the critical point. These classical EOS implicitly assume that pressure may be expanded about the critical point in a Taylor series in density and temperature; such expansion leads to the conclusion that the liquid-vapor coexistence curve is quadratic near the critical point, in disagreement with experiment. Experimentally, the compressibility along the critical isochore approaches infinity at the critical point with a noninteger exponent $\gamma = 1.33$ , in disagreement with classical EOS theory where $\gamma = 1$. As pointed out,[6,7] the failure of classical EOS theory follows from neglect of long-wavelength density fluctuations. In the 1970's, Wilson[8-9] developed a renormalization-group (RG) theory using a phase-space cell approximation to incorporate contributions from long-wavelength density fluctuations. RG theory gives non-classical critical exponents in agreement with experiment. A recent high-level review of RG theory is given by Fisher.[10] However, RG theory is only valid asymptotically close to the critical point and cannot be implemented outside the critical region; it does not reduce to the ideal gas law at low density. Therefore attention has been given by several authors,[11-20] notably by Sengers,[21-23] to combine non-classical and classical theories to represent fluid properties both close-to and far-from the critical point. This work is one more effort toward that goal; however, this work is directed specifically at the properties of chain fluids. While the work discussed here may not be as rigorous as those of others, it has an important advantage: only a few adjustable parameters are required. The procedure outlined here, therefore, is promising for application to real systems where experimental data are scarce.

Based on Wilson's phase-space cell approximation, White and coworkers[24-27] developed a global RG theory that extends the range of the original RG theory and that can be applied beyond the critical region. In their work, the Helmholtz energy is divided into repulsive and attractive parts. The repulsive part does not make an appreciable contribution to the long-range correlations of a fluid; RG methods are therefore applied only to the attraction part. White's theory is expressed

in a recursion form for the Helmholtz energy density; it reproduces experimentally observed critical exponents, and is capable of describing the $pVT$ properties and phase behavior inside and near-outside the critical region for simple spherical molecules, like argon and methane.

Following White et al., Lue and Prausnitz[28,29] enhanced the accuracy and range of White's RG transformation through an improved Hamiltonian. Good representation of thermodynamic properties and phase equilibria were obtained for square-well (SW) model fluids, simple real fluids and their mixtures. A similar method was also used by Tang[30] to study the global behavior of Lennard-Jones fluids. All previous publications have been directed to fluids containing simple spherical molecules.

In recent years, remarkable progress has been made toward a classical theory for chain fluids. Hu, Liu and Prausnitz[31] established an equation of state for chain fluids (EOSCF) through an approximation of the cavity-correlation function of chains; this approach has been further adopted to study charged chain fluids that can serve as a simple model for polyelectrolytes.[32] Better known is the work of Chapman and coworkers[33-35] who developed the statistical associated fluid theory (SAFT) originally proposed by Wertheim.[36] These theories provide a molecular-based EOS retaining a relatively simple form. As shown recently,[37-47] both EOSCF and SAFT have become the most widely-used EOS for calculating phase equilibria for a wide variety of complex chain systems. However, the mean-field nature of these EOS limits their success to the region far from the critical point.

To yield better results in the critical region, some authors[44-46] have suggested rescaling the molecular parameters in the EOS to fit experimental critical constants. Although this suggestion yields a better representation of fluid behavior near the critical point, it cannot reproduce the global features (cf. Figure 2 in ref. 44). Rescaling provides a simple mathematical method but it does not incorporate density fluctuations. On the other hand, Adidharma and Radosz[47] have adopted the crossover method of Kiselev et al.[16] to improve SAFT's representation inside the critical region and indeed, better results are obtained. However, a large number of adjustable parameters is required.

The purpose of this work is to present a global EOSCF combining White's RG theory with the original EOSCF (EOSCF+RG) to represent the behavior of chain fluids outside and inside the critical region. Toward that end, we give in Sec. II expressions for the original EOSCF for a fluid of square-well chains. In Sec.III we give a EOSCF+RG equation. Sec. IV gives results for thermodynamic properties and phase equilibria of model square-well chain fluids and real $n$-alkane fluids; these results are, respectively, compared with those from computer simulation and from experiment. The last section gives some concluding remarks.

## II. EOSCF EQUATION OUTSIDE THE CRITICAL REGION

The chain fluid is represented by a freely tangent-joined SW chain with $m$ chain segments. The interaction potential between segments in the chain is given by

$$u(r) = u^{\mathrm{hs}}(r,\sigma) + u^{\mathrm{sw}}(r,\lambda) \tag{1}$$

where $r$ is the center-to-center segment distance and $u^{\mathrm{hs}}$ is a short-ranged steep hard-sphere repulsive potential, taken as a reference potential; $u^{\mathrm{sw}}$ is the perturbed SW potential:

$$u^{\mathrm{hs}}(r,\sigma) = \begin{cases} \infty & r < \sigma \\ 0 & r > \sigma \end{cases} \tag{2}$$

$$u^{\mathrm{sw}}(r,\lambda) = \begin{cases} 0 & r < \sigma \\ -\varepsilon & \sigma < r < \lambda\sigma \\ 0 & r > \lambda\sigma \end{cases} \tag{3}$$

where $\sigma$ is the segment diameter; $\lambda$ and $\varepsilon$ are, respectively, the reduced width and depth of the SW interaction potential.

Without loss of generality, but with a view towards fitting experimental data, we assume that $\varepsilon$ depends on temperature $T$ as proposed by Chen and Kreglewski,[48]

$$\varepsilon = \varepsilon_0(1 + e/k_{\mathrm{B}}T) \tag{4}$$

where $\varepsilon_0$ and $e$ are constants; $k_{\mathrm{B}}$ is Boltzmann constant. Interaction parameter $\varepsilon$ is for segments (not for molecules); Following Huang and Radosz,[40] we set $e/k_{\mathrm{B}} = 5\mathrm{K}$ throughout. Following Barker-Henderson (BH) theory,[49] the temperature dependence of the effective diameter $\sigma$ is

$$\sigma = \sigma_0[1 - C\exp(-3\beta\varepsilon_0)] \tag{5}$$

where $\sigma_0$ is a temperature-independent diameter and $\beta = 1/k_{\mathrm{B}}T$. $C$ is an integration constant; following Chen and Kreglewski,[48] we set $C = 0.12$.

The Helmholtz energy density $f$, i.e., the Helmholtz energy per unit of volume $V$, is obtained from the general form of the EOSCF[31,32]

$$f^{\mathrm{EOSCF}} = f^{\mathrm{id}} + f^{\mathrm{hs}} + f^{\mathrm{sw}} + f^{\mathrm{chain}}. \tag{6}$$

The contribution of the ideal gas is given by

$$f^{\mathrm{id}} = k_{\mathrm{B}}T[\rho\ln(\rho\Lambda^3) - \rho] \tag{7}$$

where $\rho$ is the number density of molecules, and $\Lambda$ denotes the de Broglie thermal wavelength depending only on temperature and molecular mass.

The hard-sphere interaction is given by the Carnahan-Starling equation[50]

$$f^{\mathrm{hs}} = k_{\mathrm{B}} T m\rho \frac{4\eta - 3\eta^2}{(1-\eta)^2} \tag{8}$$

where $\eta$ is the packing fraction defined by

$$\eta = \frac{\pi}{6} m\rho\sigma^3 . \tag{9}$$

For the contribution from the perturbation SW potential, we adopt the second-order BH perturbation theory[49,51,52] that follows from the high-temperature expansion of Zwanzig,[53]

$$f^{\mathrm{sw}} = m\rho(a_1 + \beta a_2) . \tag{10}$$

The mean-attractive energy $a_1$ is given by a compact expression from the mean-value theorem,[54]

$$a_1 = -4\eta\varepsilon(\lambda^3 - 1) g^{\mathrm{hs}}(\sigma, \eta_{\mathrm{eff}}) \tag{11}$$

where the contact value of the pair correlation function for hard spheres is estimated at an effective packing fraction $\eta_{\mathrm{eff}}$,

$$g^{\mathrm{hs}}(\sigma, \eta_{\mathrm{eff}}) = \frac{1 - \eta_{\mathrm{eff}}/2}{(1-\eta_{\mathrm{eff}})^3} \tag{12}$$

with

$$\eta_{\mathrm{eff}} = c_1\eta + c_2\eta^2 + c_3\eta^3 . \tag{13}$$

Coefficients $c_n$ are calculated by the matrix[54]

$$\begin{pmatrix} c_1 \\ c_2 \\ c_3 \end{pmatrix} = \begin{pmatrix} 2.25855 & -1.50349 & 0.249434 \\ -0.669270 & 1.40049 & -0.827739 \\ 10.1576 & -15.0427 & 5.30827 \end{pmatrix} \begin{pmatrix} 1 \\ \lambda \\ \lambda^2 \end{pmatrix} \tag{14}$$

The second perturbation term $a_2$ describing fluctuations of the attractive energy is given by

$$a_2 = \frac{(1-\eta)^4 \varepsilon}{2(1+4\eta+4\eta^2)} \frac{\partial a_1}{\partial \eta} . \tag{15}$$

Eqs.(8) and (10) refer to monomers, not chain molecules. It is necessary to include a chain term to correct for chain connectivity. Following previous work,[31,32] the cavity-correlation function of chains can be approximated as the product of two contributions: a chemical contribution $(1-\alpha)^m$ dependent on the degree of association $\alpha$, and a physical contribution expressed by the product of nearest-neighbor effective two-particle cavity-correlation function $y_{ij}^{\mathrm{eff}}(j = i+1)$:

$$y_{12\cdots m}^{m}(r_{12}, r_{23}, \ldots r_{m-1,m}) = (1-\alpha)^m \prod_{\substack{i=1 \\ j=i+1}}^{m-1} y_{ij}^{\mathrm{eff}}(r_{ij}) \tag{16}$$

where $y_{ij}^{\text{eff}}(j=i+1)$ in this work is the cavity correlation function for SW monomers at contact:

$$y^{\text{sw}}(\sigma)=g^{\text{sw}}(\sigma)\exp(-\varepsilon/k_{\text{B}}T) \tag{17}$$

$$g^{\text{sw}}(\sigma)=\frac{1-\eta/2}{(1-\eta)^3}+\frac{\beta}{4}\left(\frac{\partial a_1}{\partial\eta}-\frac{\lambda}{3\eta}\frac{\partial a_1}{\partial\lambda}\right). \tag{18}$$

When $\alpha=1$, the Helmholtz energy due to chain connectivity can be derived as,

$$f^{\text{chain}}=k_{\text{B}}T\rho(1-m)\ln y^{\text{sw}}(\sigma). \tag{19}$$

In Eq.(19), if $y^{\text{sw}}(\sigma)$ is replaced by $y^{\text{hs}}(\sigma)$, i.e., the contact value of the cavity correlation function for hard spheres, the above EOSCF reduces to the original SAFT[33-35] equation. Figure 1 compares EOSCF and SAFT with computer simulation results[55] for SW chain with $m=4$ and $\lambda=1.5$ where $T^*=1/\beta\varepsilon$ is reduced temperature. $y_{\text{hs}}$ denotes SAFT; sw1 refers to EOSCF with the first-order SW term ($a_2=0$), in contrast to sw2 that includes also the second-order SW term. As expected, EOSCF is better than SAFT; EOSCF-sw2 performs somewhat better than EOSCF-sw1, but all are seriously inadequate inside the critical region.

## III. EOSCF+RG EQUATION INSIDE THE CRITICAL REGION

Far from the critical point, conventional (classical) theories perform well because the correlation length is small; only correlations between a few near-by molecules contribute significantly to the Helmholtz energy. However, approaching the critical point, the correlation length increases, and long-wavelength density fluctuations become important, diverging to infinity at the critical point. Large correlation lengths imply that the system is not homogeneous near the critical point; correlations between larger and larger numbers of molecules make an increasingly significant contribution to the Helmholtz energy. Because most mean-field theories are not able to describe accurately correlations between large numbers of molecules, they perform poorly in the critical regime where RG theory provides the only known way to yield correct fluid behavior. Wilson's phase-space cell approximation takes into account fluctuations successively with larger and larger length scales, up to the correlation length.

For an open system at temperature $T$ with particle number $N$, volume $V$ and chemical potential $\mu$, we can write the grand canonical partition function as[56]

$$\Xi=\sum_N Z(T,V,N)\exp(N\beta\mu) \tag{20}$$

where $Z(T,V,N)$ is the canonical partition function:

$$Z(T,V,N)=\frac{1}{N!\Lambda^{3N}}\int_V\cdots\int\exp[-\sum_{i\neq j}\beta u(r_i-r_j)/2]\mathrm{d}\mathbf{r}_1\cdots\mathrm{d}\mathbf{r}_N \tag{21}$$

where the integral is over all possible space. In contrast to Eq.(21), Eq.(20) can take into account fluctuations in the system. The transformation of the grand canonical partition function into a functional integral is[57]

$$\Xi=\int\tilde{D}\rho(\cdot)\tilde{D}\phi(\cdot)\Xi^{\mathrm{ref}}[i\phi]\exp\left\{\int\beta\mu\rho(r)\mathrm{d}\mathbf{r}-i\int\rho(r)\phi(r)\mathrm{d}\mathbf{r}-\tfrac{1}{2}\int\rho(r)v(r-r')\rho(r')\mathrm{d}\mathbf{r}\mathrm{d}\mathbf{r}'\right. \tag{22}$$

where $\rho(r)$ and $\phi(r)$ are integration variables; $\rho(r)$ is the instantaneous density distribution and $\phi(r)$ is the potential field; $v(r)$ is the reduced perturbed potential, here equal to $\beta u^{\mathrm{sw}}(r)$; $\Xi^{\mathrm{ref}}$ is the grand partition function for the reference fluid:

$$\Xi^{\mathrm{ref}}=\frac{\exp(N\beta\mu)}{N!\Lambda^{3N}}\int_V\cdots\int\exp[-\sum_{i\neq j}\beta u^{\mathrm{ref}}(r_i-r_j)/2]\mathrm{d}\mathbf{r}_1\cdots\mathrm{d}\mathbf{r}_N\,. \tag{23}$$

For the hard-sphere reference system considered here, we have only small contributions from density fluctuations of very short wavelengths.[58] We assume that this contribution is taken fully into account in the Helmholtz energy calculated for the reference system.

Due to a very steep repulsive potential, the potential of the reference system does not affect the fluctuations of long wavelengths. However, the attractive intermolecular interaction of limited range (in this work, the SW perturbation potential) can have a strong effect on long-wavelength density fluctuations. For our purposes, only the contribution from SW attraction is required. Following White et al.[24-27], we incorporate density fluctuations of all wavelengths, including short wavelengths and those that are asymptotically long.

We first divide the contributions from the attractive potential into two parts, a short-wavelength part $v^s$, and a long-wavelength part $v^l$,[59-61]

$$\hat{v}^{-1}(q)=\hat{v}^{s^{-1}}(q)+\hat{v}^{l^{-1}}(q) \tag{24}$$

where the carets denote Fourier transforms. The choice of $v^s$ and $v^l$ is somewhat arbitrary provided that $\hat{v}^{s^{-1}}(q)$ approaches $\hat{v}^{-1}(q)$ rapidly when $q>2\pi/L$; and $\hat{v}^{l^{-1}}(q)$ approaches $\hat{v}^{-1}(q)$ rapidly when $q<2\pi/L$. It is assumed that contributions from density fluctuations of wavelengths less than cutoff length $L$ can be accurately evaluated by a mean-field theory.

Following Lue and Prausnitz,[28] we use the following long-wavelength potential,

$$\hat{v}^l(q)=-2\beta a+\beta q^2 a\varpi^2 \tag{25}$$

where $a$ is the interaction volume with unit of energy-volume and $\varpi$ refers to the range of the attractive potential. They are given, respectively, by

$$a = -\frac{1}{2}\int u^{\mathrm{sw}}(r)\mathrm{d}\mathbf{r} = \frac{2\pi}{3}\varepsilon(\lambda\sigma)^3 \tag{26}$$

$$\varpi^2 = -\frac{1}{3!\,a}\int r^2 u^{\mathrm{sw}}(r)\mathrm{d}\mathbf{r} = \frac{1}{5}(\lambda\sigma)^2 \tag{27}$$

Because of Eq. (24), the density distribution $\rho(r)$ can be divided into two contributions, $\rho^l(r)$ corresponding primarily to long wavelengths, and $\rho^s(r)$ corresponding primarily to short wavelengths. With these new variables, Eq. (22) can be rewritten as

$$\Xi = \frac{1}{Q^l}\int \tilde{D}\rho^l(\cdot)\exp\left\{\int \beta\mu\rho^l(r)\mathrm{d}\mathbf{r} - \tfrac{1}{2}\int \rho^l(r)v^l(r-r')\rho^l(r')\mathrm{d}\mathbf{r}\mathrm{d}\mathbf{r}' - \bar{F}^s[\rho^l]\right. \tag{28}$$

where

$$\begin{aligned}\exp\{-\bar{F}^s[\rho^l]\} = \frac{Q}{Q^s}\int \tilde{D}\rho^s(\cdot)\tilde{D}\phi(\cdot)\times \Xi^{\mathrm{ref}}[i\phi]\exp\left\{\int \beta\mu\rho^s(r)\mathrm{d}\mathbf{r}\right.\\ \left. - i\int[\rho^l(r)+\rho^s(r)]\phi(r)\mathrm{d}\mathbf{r} - \tfrac{1}{2}\int \rho^s(r)v^s(r-r')\rho^s(r')\mathrm{d}\mathbf{r}\mathrm{d}\mathbf{r}'\right.\end{aligned} \tag{29}$$

$$Q = \int \tilde{D}\rho(\cdot)\exp\left\{-\tfrac{1}{2}\int \rho(r)v(r-r')\rho(r')\mathrm{d}\mathbf{r}\mathrm{d}\mathbf{r}'\right. \tag{30}$$

$$Q^l = \int \tilde{D}\rho(\cdot)\exp\left\{-\tfrac{1}{2}\int \rho(r)v^l(r-r')\rho(r')\mathrm{d}\mathbf{r}\mathrm{d}\mathbf{r}'\right. \tag{31}$$

$$Q^s = \int \tilde{D}\rho(\cdot)\exp\left\{-\tfrac{1}{2}\int \rho(r)v^s(r-r')\rho(r')\mathrm{d}\mathbf{r}\mathrm{d}\mathbf{r}'\right. \tag{32}$$

Functional $\bar{F}^s$ is the contribution from short-wavelength fluctuations alone; it may be estimated by the local-density approximation,

$$\bar{F}^s(\rho) = \int f^s(\rho)\mathrm{d}\mathbf{r} \tag{33}$$

where $f^s$ is the Helmholtz energy density for a homogeneous system with density $\rho$; $f^s$ can be calculated using mean-field theory, such as the original EOSCF equation. However, because $f^s$ only includes short-wavelength density fluctuations, we should subtract the contributions of long-wavelength fluctuations from EOSCF equation, which we approximate as $-a\rho^2$, then,

$$f^s = f^{\mathrm{EOSCF}} + a\rho^2. \tag{34}$$

This approximation gives only the contribution for the limiting case $q = 0$; more accurately, the approximation should account for contributions in the range $0 \le q < 2\pi / L$.

Substituting Eq. (33) into Eq. (28) gives

$$\Xi = \frac{1}{Q^l}\int \tilde{D}\rho^l(\cdot)\exp\left\{-\frac{a\varpi^2}{2}\int \nabla\rho^l(r)\cdot\nabla\rho^l(r)\mathrm{d}\mathbf{r} - \int\left[f^s(\rho^l(r)) - a(\rho^l(r))^2\right]\mathrm{d}\mathbf{r}\right\}. \tag{35}$$

When the system approaches the critical point where more and more molecules are coupled, longer and longer wavelengths make significant contributions; there is then no analytical solution for Eq.(35), requiring a numerical solution. We first evaluate the zero-order solution $f_0$ by the saddle-point approximation,[57]

$$f_0 = f^s - a\rho^2 \tag{36}$$

with Eq. (34), we have

$$f_0 = f^{\mathrm{EOSCF}}. \tag{37}$$

We adopt White's RG method[24-27] to incorporate the contributions from density fluctuations with longer and longer wavelengths yielding the following recursion relations to estimate the Helmholtz energy density:

$$f_n(\rho) = f_{n-1}(\rho) + \delta f_n(\rho) \tag{38}$$

$$\delta f_n(\rho) = -K_n \ln \frac{\Omega_n^s(\rho)}{\Omega_n^l(\rho)}, \qquad 0 \le \rho < \rho_{\max}/2 \tag{39.a}$$

$$\delta f_n(\rho) = 0, \qquad \rho_{\max}/2 \le \rho < \rho_{\max} \tag{39.b}$$

where $\Omega_n^l$ and $\Omega_n^s$ refer to the density fluctuations for the long-range attraction and the short-range attraction, respectively. $\rho_{\max}$ is the maximum possible molecule density indicated by $\eta = 1$ giving $\rho_{\max} = 6/\pi m\sigma^3$. Coefficient $K_n$ is defined by

$$K_n = \frac{1}{2^{3n}\beta L^3} \tag{40}$$

$$\Omega_n^\alpha(\rho) = \int_0^\rho \exp(-G_n^\alpha(\rho,x)/K_n)\mathrm{d}x, \qquad \alpha = s,l \tag{41}$$

$$2G_n^\alpha(\rho,x) = \bar{f}_n^\alpha(\rho+x) + \bar{f}_n^\alpha(\rho-x) - 2\bar{f}_n^\alpha(\rho), \qquad \alpha = s,l \tag{42}$$

$$\bar{f}_n^l(\rho) = f_{n-1}(\rho) + a\rho^2 \tag{43}$$

$$\bar{f}_n^s(\rho) = f_{n-1}(\rho) + a\rho^2 \frac{\Phi\varpi^2}{2^{2n+1}L^2}. \tag{44}$$

Parameter $\Phi$ is the average gradient of the wavelet function $\psi(r)$; the recursion relations are established in terms of $\Phi$.[62]

$$\Phi = \int \nabla\psi(r)\cdot\nabla\psi(r)\mathrm{d}\mathbf{r}. \tag{45}$$

$\Phi$ only depends on $\psi(r)$, not on the molecular interaction potential; therefore it is an adjustable parameter, in addition to cutoff length $L$.

The above recursion procedure can be interpreted as the calculation of the ratio of non-mean-field contributions to mean-field contributions at gradually increasing by long wavelengths. We perform the calculations numerically with a density step $\rho_{\max}/500$, and smooth the resulting Helmholtz energy density by a cubic spline function. In principle, the recursion should be performed until $n$ approaches infinity; however, in our calculation we find that $n=5$ is sufficient to obtain good final results.

After we calculate the Helmholtz energy of the system, the chemical potential and pressure are obtained by

$$\mu = \left(\frac{\partial f}{\partial \rho}\right)_{T,V} \tag{46}$$

$$P = \rho\mu - f \tag{47}$$

and the critical point can be evaluated from the standard critical criteria:

$$\begin{cases} \left(\dfrac{\partial P}{\partial V}\right)_T = 0 \\ \left(\dfrac{\partial^2 P}{\partial V^2}\right)_T = 0 \end{cases} \tag{48}$$

## IV. RESULTS AND DISCUSSION

### Square-well chain fluids

Before applying our above-described EOSCF+RG theory to practical systems, we compare our theory for model square-well chain fluids to results obtained by computer simulation. We consider SW chains with width $\lambda = 1.5$ because there are several systematical studies[55,63,64] for this case. We set the cutoff length $L = 2\sigma$ and choose $\Phi$ to fit the simulated critical temperature. Table I presents $\Phi$, reduced critical temperature $T_c^*$ and critical packing fraction $\eta_c$ for SW chains with length $m = 1$, 2, 4, 8, 16 estimated from simulation, EOSCF and EOSCF+RG. As expected, EOSCF overestimates $T_c^*$ but underestimates $\eta_c$. Although we adjust $\Phi$ only to fit $T_c^*$ but not $\eta_c$, EOSCF+RG gives good predictions for $\eta_c$. Optimized $\Phi$ rises with chain length. Critical pressures are not presented here because they were not calculated by simulation except for $m = 1$.

Figure 2 shows vapor-liquid coexistence curves for several square-well chain fluids. The circles are computer simulation results;[55,63,64] the dashed lines are predictions from EOSCF and the solid lines are those from EOSCF+RG. For $m = 1$, EOSCF underestimates the saturated liquid

density exhibiting a narrower coexistence curve. With rising chain length, EOSCF overestimates the saturated liquid density but underestimates the saturated vapor density, and the coexistence curve becomes broader. Outside the critical region, EOSCF+RG theory gives results similar to those from EOSCF. However, after incorporating contributions from long-wavelength fluctuations, EOSCF+RG shows large improvement inside the critical region where EOSCF fails. The longer the chain length, the greater the deviations for both EOSCF and EOSCF+RG from the simulation "experiments", especially for EOSCF. This result suggests that more effort is required to describe chain fluids. EOSCF theory is a first-order thermodynamic perturbation theory (TPT1) that accounts only for the correlations between nearest-neighbor segments in the chain, but not for higher correlations between other in-chain segments. However, suggestions for such revision are provided by Hu's work[31], SAFT-D,[64] TPT-D[66], TPT2[67].

**Real fluids: *n*-alkanes**

The thermodynamic properties and phase behavior of *n*-alkanes are of particular interest in the fossil-fuel industries. We model *n*-alkanes as square-well chain fluids and examine the capability of EOSCF+RG theory to describe their thermodynamic properties. The square-well segment-segment parameters for methane ($C_1$) to *n*-eicosane ($C_{20}$) are determined as follows. Because the carbon-carbon bond length for *n*-alkanes is about 1/3 of the diameter of $CH_4$, a simple empirical relation between chain length $m$ and carbon number C is $m = 1 + (C-1)/3$.[68,69] Parameters for the interaction potential $\varepsilon_0$, segment diameter $\sigma_0$ and interaction width $\lambda$ are optimized to fit the experimental data outside the critical region. For $C_1$ to $C_4$, we used experimental vapor pressures and saturated liquid densities[70,71] at temperatures 20% below critical temperature $T_c$, and experimental isotherms ($pVT$)[71] at temperatures 20% above $T_c$. For $C_5$ to $C_{20}$, we used vapor pressures and saturated liquid densities[70-72] at temperatures 20% below $T_c$. To incorporate contributions from long-wavelength density fluctuations inside the critical region, we set the cutoff length $L = 11.5$ Å and select a suitable parameter $\Phi$ to fit the measured $T_c$. If the resulting critical pressure $P_c$ does not agree with that measured, we change the parameters and fit again. Table II lists the optimized segment-segment parameters.

Compared with the others, $C_1$ exhibits anomalous behavior with extremely low $\varepsilon_0$ but a higher $\Phi$ than those for $C_2$. The interaction potential $\varepsilon_0$, segment diameter $\sigma_0$, interaction width $\lambda$ and average gradient $\Phi$ tend toward asymptotic constant values upon increasing the carbon number.

Figure 3 shows the optimized square-well segment-segment parameters for $C_1$ to $C_{20}$ as a function of molecular weight Mw. Except $CH_4$, these parameters are well behaved and can be expressed by linear functions of Mw as:

$$m = 0.6190 + 0.0238\text{Mw} \tag{49.a}$$

$$m\varepsilon_0 / k = 93.5976 + 4.6987\text{Mw} \tag{49.b}$$

$$m\sigma_0^3 = 19.4039 + 1.6399\text{Mw} \tag{49.c}$$

$$m\lambda = 0.8903 + 0.0429\text{Mw} \tag{49.d}$$

$$m\Phi = 0.1151 + 0.2711\text{Mw} \tag{49.e}$$

As discussed below, such relations are useful for extrapolating to heavier *n*-alkanes where experimental data are rare.

Table III gives measured[73-75] $T_c$, $P_c$ and critical density $\rho_c$ and those predicted from EOSCF and EOSCF+RG, respectively, for $C_1$ to $C_{20}$. As expected, EOSCF overestimates $T_c$ and $P_c$ and underestimates $\rho_c$. By contrast, EOSCF+RG gives satisfactory results.

Figure 4 shows vapor-liquid coexistence curves for several *n*-alkanes from $C_1$ up to $C_{20}$. The circles are experimental data,[70,71] while the dashed and solid lines are from EOSCF and EOSCF+RG, respectively. Because EOSCF gives an incorrectly high critical temperature, EOSCF cannot predict the correct phase behavior inside the critical region; however, EOSCF+RG repairs this inadequacy because density fluctuations are reasonably incorporated. Outside the critical region, EOSCF+RG theory reduces to the original EOSCF where the latter is reliable. In general, EOSCF+RG gives good agreement with experiment in both regions.

Figure 5 shows vapor pressures for several *n*-alkanes from $C_1$ to $C_{20}$. For each fluid, EOSCF overestimates both the critical temperature and critical pressure. Below the observed critical temperature, EOSCF underestimates the vapor pressure. However, good agreement with experiment is observed for EOSCF+RG. Figure 6 shows a Clausius-Clapeyron plot where ln*P* is given as a function of 1/*T*.

Based on the linear functions Eqs. (49.a)-(49.e), we extrapolate the segment-segment parameters for heavier *n*-alkanes, as shown in Table IV, from docosane ($C_{22}$) to hexatriacontane ($C_{36}$). Table V gives the corresponding predicted critical constants from EOSCF+RG and EOSCF,

respectively. Satisfactory predictions are found from EOSCF+RG when compared with limited measured or estimated data[74-76].

Figures 7, 8 and 9 show the critical temperature $T_c$, pressure $P_c$ and critical density $\rho_c$ as functions of carbon number from $C_1$ up to $C_{36}$.

Finally, Figures 10, 11, 12 and 13 show supercritical isotherms for $CH_4$, $C_2H_6$, $C_3H_8$ and $n$-$C_4H_8$, respectively. In general, EOSCF+RG theory gives reliable $pVT$ properties for density up to $1.4\rho_c$; it gives better results than those of EOSCF, especially near the critical temperature. However, at high temperatures, both EOSCF+RG and EOSCF nearly coincide. At very high densities, significant deviations from experiment are observed for both. These deviation may result from the inadequate description of EOSCF for chain fluids or from the rough approximation in Eq. (34) but not from the RG method itself. On the other hand, it may be that accurate representation of the properties of $n$-alkanes at high densities requires consideration of many-body interactions[77-80] in addition to two-body interactions.

## V. CONCLUSION

Combining the original EOSCF with a global RG, we have developed a relatively simple crossover EOSCF+RG theory that is able to describe the properties of chain fluids both inside and outside the critical regions. Outside the critical region, where the correlation length is small, the RG correction is negligible and EOSCF+RG reduces to the original EOSCF. However, inside the critical region, the original EOSCF fails due to its mean-field nature. Accounting for the contributions from long-wavelength fluctuations, the inadequacy of EOSCF can be significantly reduced by EOSCF+RG.

We apply EOSCF+RG to $n$-alkanes modeled as square-well chain fluids. The segment-segment parameters for $C_1$ to $C_{20}$ are correlated by fitting EOSCF results to experimental vapor pressures and saturated liquid densities outside the critical region. Two additional parameters in EOSCF+RG are chosen to represent experimentally observed critical temperature and critical pressure. Starting with $C_2H_6$, linear relations exist between the segment-segment parameters and molecular weight. For heavier $n$-alkanes from $C_{22}$ to $C_{36}$, the extrapolated segment-segment parameters give good predictions of critical properties. Although the real systems studied here are $n$-alkane oligomers, for polymers like polyethylene, polypropylene and polystyrene etc, the expressions of thermodynamic properties provided above are identical and can be used directly.

In general, EOSCF+RG theory gives satisfactory critical constants, phase equilibria and *pVT* isotherms, much better than those from original EOSCF, especially near the critical point. Deviations from experiment for *pVT* isotherms at high densities are not due to the RG method; rather, they follow from other inadequacies: neglect of higher-order correlations between the segments in the chain (because EOSCF is a first-order perturbation theory) and from our rough approximation to subtract contributions from long-wavelength density fluctuations in EOSCF; and, perhaps, from many-body interactions that are not taken into account.

## ACKNOWLEDGMENTS

This work was supported by the Director, Office of Energy Research, Office of Basic Energy Sciences, Chemical Sciences Division of the U.S. Department of Energy, under Contract DE-AC03-76SF00098. Additional support by the Chinese National Science Foundation is acknowledged. J.W.J. wishes to thank Dr. Leo Lue and Prof. John White for enlightening discussions, and Dr. G. Jackson for providing the preprints of his work.

1 J. M. Prausnitz, R. N. Lichtenthaler and E. G. de Azevedo, *Molecular Thermodynamics of Fluid Phase Equilibria*, 3rd ed. (Prentice-Hall, Englewood Cliffs, New Jersey, 1999).

2 R. J. Sadus, *High Pressure Phase Behavior of Multicomponent Fluid Mixtures* (Elsevier Sci., Netherlands, 1992).

3 J. D. van der Waals, Thesis, University of Leiden, 1873; English translation and introductory essay by J. S. Rowlinson, 1988, *On the Continuity of Gaseous and Liquid States*, Studies in Statistical Mechanics, Vol.**14** (North Holland, Amsterdam).

4 O. Redlich and J. N. S. Kwong, Chem. Rev. **44**, 233 (1949).

5 D. Y. Peng and D. B. Robinson, Ind. Eng. Chem. Fundam. **15**, 59 (1976).

6 J. V. Sengers and J. M. H. L. Sengers, Annu. Rev. Phys. Chem. 37, 189 (1986).

7 J. M. H. L. Sengers, in *Supercritical Fluid Technology Reviews in Modern Theory and Applications*, Eds. T. J. Bruno and J. F. Ely (CRC Press, Boca Raton, 1991).

8 K. G. Wilson, Phys. Rev. B **4**, 3174, 3184 (1971).

9 K. G. Wilson and M. E. Fisher, Phys. Rev. Lett. **28**, 240 (1972).

10 M. E. Fisher, Rev. Mod. Phys., **70**, 653 (1998).

11 J. Fox, J. Stat. Phys. **21**, 243 (1979). Fluid Phase Equil. **14**, 45 (1983).

12 D. D. Erickson and T. W. Leland, Int. J. Thermophys. **7**, 911 (1986).

13 J. J. de Pablo and J. M. Prausnitz, Fluid Phase Equil. **50**, 101 (1989)

14 J. J. de Pablo and J. M. Prausnitz, Fluid Phase Equil. **59**, 1 (1990).

15 S. B. Kiselev, High Temp. **26**, 337 (1988); **28**, 42 (1990).

16 S. B. Kiselev, Fluid Phase Equil. **147**, 7 (1998).

17 M. Yu. Belyakov, S. B. Kiselev, and J. C. Rainwater, J. Chem. Phys. **107**, 3085 (1997).

18 A. Parola and L. Reatto, Phys. Rev. Lett. **53**, 2417 (1984).

19 A. Parola and L. Reatto, Phys. Rev. A **31**, 3309 (1985).

20 A. Meroni, A. Parola, and L. Reatto, Phys. Rev. A **42**, 6104 (1990).

21 P. C. Albright, J. V. Sengers, J. F. Nicoll and M. Ley-Koo, Int. J. Thermophys. **7**, 75 (1986).

22 A. A. Povodyrev, M. A. Anisimov, J. V. Sengers and J. M. H. L. Sengers, Physica A, **244**, 298 (1997).

23 T. A. Edison, M. A. Anisimov and J. V. Sengers, Fluid Phase Equil., **151**, 429 (1998).

24 J. A. White, Fluid Phase Equil. **75**, 53 (1992).

25 L. W. Salvino and J. A. White, J. Chem. Phys. **96**, 4559 (1992).

26 J. A. White and S. Zhang, J. Chem. Phys. **99**, 2012 (1993); **103**, 1922 (1995).

27 J. A. White and S. Zhang, Int. J. Thermophys. **19**, 1019 (1998)

28 L. Lue and J. M. Prausnitz, J. Chem. Phys. **108**, 5529 (1998).

29 L. Lue and J. M. Prausnitz, AIChE J. **44**, 1455 (1998).

30 Y. Tang, J. Chem. Phys. **109**, 5935 (1998).

31 Y. Hu, H. L. Liu and J. M. Prausnitz, J. Chem. Phys. **104**, 396 (1996).

32 J. W. Jiang, H. L. Liu, Y. Hu and J. M. Prausnitz, J. Chem. Phys. **108**, 780 (1998).

33 G. Jackson, W. G. Chapman and K. E. Gubbins, Mol. Phys. **65**, 1 (1988).

34 W. G. Chapman, G. Jackson and K. E. Gubbins, Mol. Phys. **65**, 1057 (1988).

35 W. G. Chapman, K. E. Gubbins, G. Jackson and M. Radosz, Ind. Eng. Chem. Res. **29**, 1709 (1990).

36 M. S. Wertheim, J. Stat. Phys. **42**, 459, 477 (1986).

37 H. L. Liu and Y. Hu, Fluid Phase Equil. **122**, 75 (1996); **138**, 69 (1997); **151**, 667 (1998).

38 H. L. Liu and Y. Hu, Ind. Eng. Chem. Res. **37**, 3058 (1998).

39 J. W. Jiang, H. L. Liu and Y. Hu, J. Chem. Phys. **110**, 4952 (1999).

40 S. H. Huang and M. Radosz, Ind. Eng. Chem. Res. **29**, 2284 (1990); **30**, 1994 (1991).

41 P. J. Smits, I. G. Economou, C. J. Peters and J. D. Arons, J. Phys. Chem. **98**, 12080 (1994).

42 M. N. G-Lisbona, A. Galindo, G. Jackson and A. N. Burgess, J. Amer. Chem. Soc. **120**, 4191 (1998).

43 A. Galindo, A. Gil-Villegas, G. Jackson, and A. N. Burgess, 16$^{th}$ Thermodynamics (London, 1999).

44 A. Galindo, P. J. Whitehead, G. Jackson and A. N. Burgess, J. Phys. Chem. **100**, 6781 (1996).

45 C. McCabe, G. Jackson, Phys. Chem. Chem. Phys. **1**, 2057 (1999).

46 F. J. Blas and L. F. Vega, J. Chem. Phys. **109**, 7405 (1998).

47 H. Adidharma and and M. Radosz, Ind. Eng. Chem. Res. **37**, 4453 (1998).

48 S. S. Chen and A. Kreglewski, Ber. Bunsen-Ges. Phys. Chem. **81**, 1048 (1977).

49 J. A. Barker and D. Henderson, J. Chem. Phys. **47**, 2856, 4714 (1967).

50 N. F. Carnahan and K. E. Starling, J. Chem. Phys. **51**, 635 (1969).

51 J. A. Barker and D. Henderson, Annu. Rev. Phys. Chem. **23**, 439 (1972).

52 J. A. Barker and D. Henderson, Rev. Mod. Phys. **48**, 587 (1975).

53 R. W. Zwanzig, J. Chem. Phys. **22**, 1420 (1954).

54 A. Gil-Villegas, A. Galindo, P. J. Whitehead, S. J. Mills, G. Jackson and A. N. Burgess, J. Chem. Phys. **106**, 4168 (1997).

55 F. A. Escobedo and J. J. de Pablo, Mol. Phys. **87**, 347 (1996).

56 J. P. Hansen and I. R. McDonald, *Theory of Simple Fluids* (Academic, Boston, 1986).

57 J. W. Negele and H. Orland, *Quantum Many-Particle Systems* (Addison-Wesley, CA, 1988).

58 J. D. Weeks, D. Chandler, and H. C. Andersen, J. Chem. Phys. **54**, 5237 (1971).

59 Yu. M. Ivanchenko and A. A. Lisyansky, *Physics of Critical Fluctuations* (Springer, New York, 1995).

60 Yu. M. Ivanchenko and A. A. Lisyansky, Phys. Rev. A **45**, 8525 (1992).

61 Yu. M. Ivanchenko, A. A. Lisyansky, and A. A. Filippov, J. Stat. Phys. **66**, 1139 (1992).

62 G. Battle, in *Recent Advances in Wavelet Analysis*, Eds. L. L. Schumaker and G. Webb (Academic Press, Boston, 1994).

63 L. Vega, E. de Miguel, L. F. Rull, G. Jackson and I. A. McLure, J. Chem. Phys. **96**, 2296 (1992).

64 A. Yethiraj and C. K. Hall, Mol. Phys. **72**, 619 (1991).

65 D. Ghonasgi and W. G. Chapman, J. Chem. Phys. **100**, 6633 (1994).

66 J. Chang and S. I. Sandler, Chem. Eng. Sci. **49**, 2777 (1994).

67 M. S. Wertheim, J. Chem. Phys. **85**, 2929 (1986); **87**, 7323 (1987); **88**, 1145, 1214 (1988).

68 G. Jackson and K. E. Gubbins, Pure Appl. Chem. **61**, 1021 (1989).

69 A. L. Archer, M. D. Amos, G. Jackson and I. A. McLure, Int. J. Thermophys. **17**, 201 (1996).

70 B. D. Smith and R. Srivastava, *Thermodyanmic Data for Pure Compounds* (Elsevier, Amsterdam, 1986).

71 N. B. Vargaftik, *Handbook of Physical Properties of Liquids and Gases*, 2nd ed. (Hemisphere Publishing Corp., Washington, 1983).

72 D. L. Morgan and R. Kobayashi, Fluid Phase Equili. **97**, 211 (1994).

73 C. Tsonopoulos, AIChE J. **33**, 2080 (1987).

74 D. Ambrose and C. Tsonopoulos, J. Chem. Eng. Data, **40**, 531 (1995).

75 D. J. Rosenthal and A. S. Teja, AIChE J. **35**, 1829 (1989).

76 K. A. M. Gasem and R. L. Robinson Jr., Fluid Phase Equili. **58**, 13 (1990).

77 J. A. Barker, C. H. J. Johnson and T. H. Spurling, Aust. J. Chem. **25**, 1811, 1813 (1972).

78 M. J. Elrod and R. J. Saykally, Chem. Rev. **94**, 1975 (1994).

79 R. J. Sadus and J. M. Prausnitz, J. Chem. Phys. **104**, 4784 (1996).

80 R. J. Sadus, Fluid Phase Equili. **144**, 351 (1998).

TABLE I. Critical constants for several square-well chain fluids. The reduced square-well width $\lambda = 1.5$; the cutoff length $L = 2\sigma$. [a]: from ref. 63; [b]: from ref. 64; [c]: from ref. 55.

| $m$ | $T_c^*$ | $\eta_c$ | $T_c^*$ | $\eta_c$ | $T_c^*$ | $\eta_c$ | $\Phi$ |
|---|---|---|---|---|---|---|---|
| | Simulation | | EOSCF | | EOSCF+RG | | |
| 1 | 1.22 [a] | 0.157 | 1.33 | 0.138 | 1.22 | 0.153 | 12.0 |
| 2 | 1.59 [b] | 0.147 | 1.74 | 0.137 | 1.58 | 0.144 | 12.0 |
| 4 | 1.90 [c] | 0.134 | 2.14 | 0.131 | 1.91 | 0.132 | 13.2 |
| 8 | 2.13 [c] | 0.12 | 2.47 | 0.114 | 2.15 | 0.117 | 13.3 |
| 16 | 2.33 [c] | 0.11 | 2.72 | 0.091 | 2.33 | 0.108 | 13.8 |

TABLE II. Optimized square-well segment-segment parameters and $\Phi$ for $n$-alkanes (from $C_1$ to $C_{20}$).

| $n$-alkane | $m$ | $\varepsilon_0 / k$ (K) | $\sigma_0$ (Å) | $\lambda$ | $\Phi$ |
|---|---|---|---|---|---|
| $CH_4$ | 1.00 | 133.14 | 3.591 | 1.575 | 6.96 |
| $C_2H_6$ | 1.33 | 173.91 | 3.710 | 1.634 | 6.16 |
| $C_3H_8$ | 1.67 | 180.38 | 3.800 | 1.665 | 7.40 |
| $C_4H_{10}$ | 2.00 | 183.68 | 3.853 | 1.690 | 7.83 |
| $C_5H_{12}$ | 2.33 | 186.32 | 3.903 | 1.703 | 8.38 |
| $C_6H_{14}$ | 2.67 | 187.15 | 3.921 | 1.716 | 8.74 |
| $C_7H_{16}$ | 3.00 | 187.63 | 3.940 | 1.728 | 9.00 |
| $C_8H_{18}$ | 3.33 | 188.82 | 3.950 | 1.733 | 9.39 |
| $C_9H_{20}$ | 3.67 | 189.59 | 3.967 | 1.738 | 9.54 |
| $C_{10}H_{22}$ | 4.00 | 190.20 | 3.981 | 1.745 | 9.65 |
| $C_{12}H_{26}$ | 4.67 | 191.23 | 3.998 | 1.753 | 9.90 |
| $C_{14}H_{30}$ | 5.33 | 191.99 | 4.011 | 1.759 | 10.08 |
| $C_{16}H_{34}$ | 6.00 | 192.58 | 4.021 | 1.764 | 10.25 |
| $C_{18}H_{38}$ | 6.67 | 193.06 | 4.029 | 1.767 | 10.35 |
| $C_{20}H_{42}$ | 7.33 | 193.45 | 4.035 | 1.770 | 10.44 |

TABLE III. Critical constants for *n*-alkanes (from $C_1$ to $C_{20}$) from experiment (ref. 73-75), from EOSCF and from EOSCF+RG.

| *n*-alkane | $T_c$ (K) | | | $P_c$ (MPa) | | | $\rho_c$ (mol/dm$^3$) | | |
|---|---|---|---|---|---|---|---|---|---|
| | Exp. | EOSCF+RG | EOSCF | Exp. | EOSCF+RG | EOSCF | Exp. | EOSCF+RG | EOSC |
| $CH_4$ | 190.6 | 190.4 | 203.7 | 4.60 | 4.57 | 6.25 | 10.16 | 10.34 | 9.17 |
| $C_2H_6$ | 305.5 | 305.8 | 331.3 | 4.91 | 4.87 | 6.90 | 7.07 | 7.07 | 6.27 |
| $C_3H_8$ | 370.0 | 369.9 | 400.3 | 4.26 | 4.29 | 6.28 | 5.11 | 5.32 | 4.69 |
| $C_4H_{10}$ | 425.2 | 424.6 | 460.3 | 3.80 | 3.83 | 5.79 | 3.93 | 4.22 | 3.73 |
| $C_5H_{12}$ | 470.4 | 469.5 | 510.4 | 3.37 | 3.40 | 5.29 | 3.23 | 3.49 | 3.05 |
| $C_6H_{14}$ | 507.9 | 507.0 | 552.8 | 3.03 | 3.08 | 4.91 | 2.73 | 3.01 | 2.60 |
| $C_7H_{16}$ | 539.7 | 539.7 | 590.2 | 2.74 | 2.79 | 4.54 | 2.34 | 2.60 | 2.24 |
| $C_8H_{18}$ | 569.4 | 568.4 | 623.3 | 2.50 | 2.58 | 4.24 | 2.04 | 2.31 | 1.97 |
| $C_9H_{20}$ | 594.6 | 593.3 | 651.6 | 2.29 | 2.40 | 3.94 | 1.84 | 2.02 | 1.74 |
| $C_{10}H_{22}$ | 617.9 | 618.3 | 681.3 | 2.12 | 2.21 | 3.68 | 1.66 | 1.86 | 1.56 |
| $C_{12}H_{26}$ | 658.2 | 658.8 | 729.6 | 1.82 | 1.92 | 3.25 | 1.39 | 1.51 | 1.29 |
| $C_{14}H_{30}$ | 693.6 | 692.7 | 770.1 | 1.62 | 1.68 | 2.89 | 1.21 | 1.32 | 1.09 |
| $C_{16}H_{34}$ | 722.6 | 720.7 | 805.6 | 1.42 | 1.45 | 2.60 | 1.06 | 1.15 | 0.93 |
| $C_{18}H_{38}$ | 747.7 | 745.1 | 834.8 | 1.32 | 1.30 | 2.36 | 0.94 | 1.01 | 0.82 |
| $C_{20}H_{42}$ | 767.5 | 765.8 | 861.6 | 1.11 | 1.13 | 2.15 | 0.85 | 0.91 | 0.72 |

TABLE IV. Extrapolated square-well segment-segment parameters and $\Phi$ for heavy $n$-alkanes from Eqs.(49).

| $n$-alkane | $m$ | $\varepsilon_0 / k$ (K) | $\sigma_0$ (Å) | $\lambda$ | $\Phi$ |
|---|---|---|---|---|---|
| $C_{22}H_{46}$ | 8.00 | 193.77 | 4.041 | 1.774 | 10.52 |
| $C_{24}H_{50}$ | 8.67 | 194.05 | 4.045 | 1.776 | 10.59 |
| $C_{28}H_{58}$ | 10.00 | 194.49 | 4.052 | 1.779 | 10.69 |
| $C_{30}H_{62}$ | 10.67 | 194.67 | 4.055 | 1.781 | 10.74 |
| $C_{32}H_{66}$ | 11.33 | 194.82 | 4.058 | 1.782 | 10.77 |
| $C_{36}H_{74}$ | 12.67 | 195.10 | 4.062 | 1.784 | 10.84 |

TABLE V. Critical constants for heavy *n*-alkanes from experiment (ref. 74-76), from EOSCF and from EOSCF+RG. Experimental critical densities are not available.

| *n*-alkanes | $T_c$ (K) | | | $P_c$ (MPa) | | | $\rho_c$ (mol/dm$^3$) | |
|---|---|---|---|---|---|---|---|---|
| | Exp. | EOSCF+RG | EOSCF | Exp. | EOSCF+RG | EOSCF | EOSCF+RG | EOSCF |
| $C_{22}H_{46}$ | 785.6 | 784.7 | 887.8 | 0.98 | 0.99 | 1.97 | 0.82 | 0.65 |
| $C_{24}H_{50}$ | 799.8 | 800.6 | 908.8 | 0.87 | 0.88 | 1.82 | 0.73 | 0.58 |
| $C_{28}H_{58}$ | 827.4 | 827.5 | 945.1 | 0.66 | 0.68 | 1.57 | 0.65 | 0.48 |
| $C_{30}H_{62}$ | 838.3 | 840.2 | 962.2 | 0.59 | 0.60 | 1.46 | 0.59 | 0.45 |
| $C_{32}H_{66}$ | 847.9 | 849.8 | 976.7 | 0.53 | 0.52 | 1.37 | 0.53 | 0.41 |
| $C_{36}H_{74}$ | 864.0 | 868.4 | 1002.7 | 0.43 | 0.42 | 1.21 | 0.46 | 0.36 |

FIG. 1. Vapor-liquid equilibria for a classical square-well chain fluid with $m = 4$ and $\lambda = 1.5$. Circles: computer-simulation data (ref. 55); dotted line: SAFT; dashed line: EOSCF with the first-order SW term; solid line: EOSCF with both first and second-order SW terms. These results do not include corrections for density fluctuations.

FIG. 2. Vapor-liquid equilibria for several square-well chain fluids with $\lambda = 1.5$ and chain length $m = 1$, 2, 4, 8, 16. Circles: computer-simulation data (ref. 55, 63, 64); dashed lines: EOSCF; solid lines: EOSCF+RG.

FIG. 3. Molecular-weight dependence of square-well segment-segment parameters for *n*-alkanes.

FIG. 4. Vapor-liquid equilibria for several *n*-alkanes. Circles: experiment (ref. 68, 71); dotted lines: EOSCF; solid lines: EOSCF+RG.

FIG. 5. Vapor pressures for several *n*-alkanes. Circles: experiment (ref. 70-72); dotted lines: EOSCF; solid lines: EOSCF+RG.

FIG. 6. Clausius-Clapeyron plot: $\ln P$ as a function of $1/T$ for several *n*-alkanes. Legends as in Fig.5.

FIG. 7. Critical temperatures for *n*-alkanes. Circles: experiment (ref. 73-76); dotted lines: EOSCF; solid lines: EOSCF+RG.

FIG. 8. Critical pressures for *n*-alkanes. Legends as in Fig.7.

FIG. 9. Critical densities for *n*-alkanes. Legends as in Fig.7.

FIG. 10. Isotherms for methane at 200, 400 and 1000K. Circles: experiment (ref. 70); dotted lines: EOSCF; solid lines: EOSCF+RG.

FIG. 11. Isotherms for ethane at 310, 400 and 500K. Legends as in Fig.10.

FIG. 12. Isotherms for propane at 380, 500 and 600K. Legends as in Fig.10.

FIG. 13. Isotherms for *n*-butane at 430, 500 and 600K. Legends as in Fig.10.

Fig.1

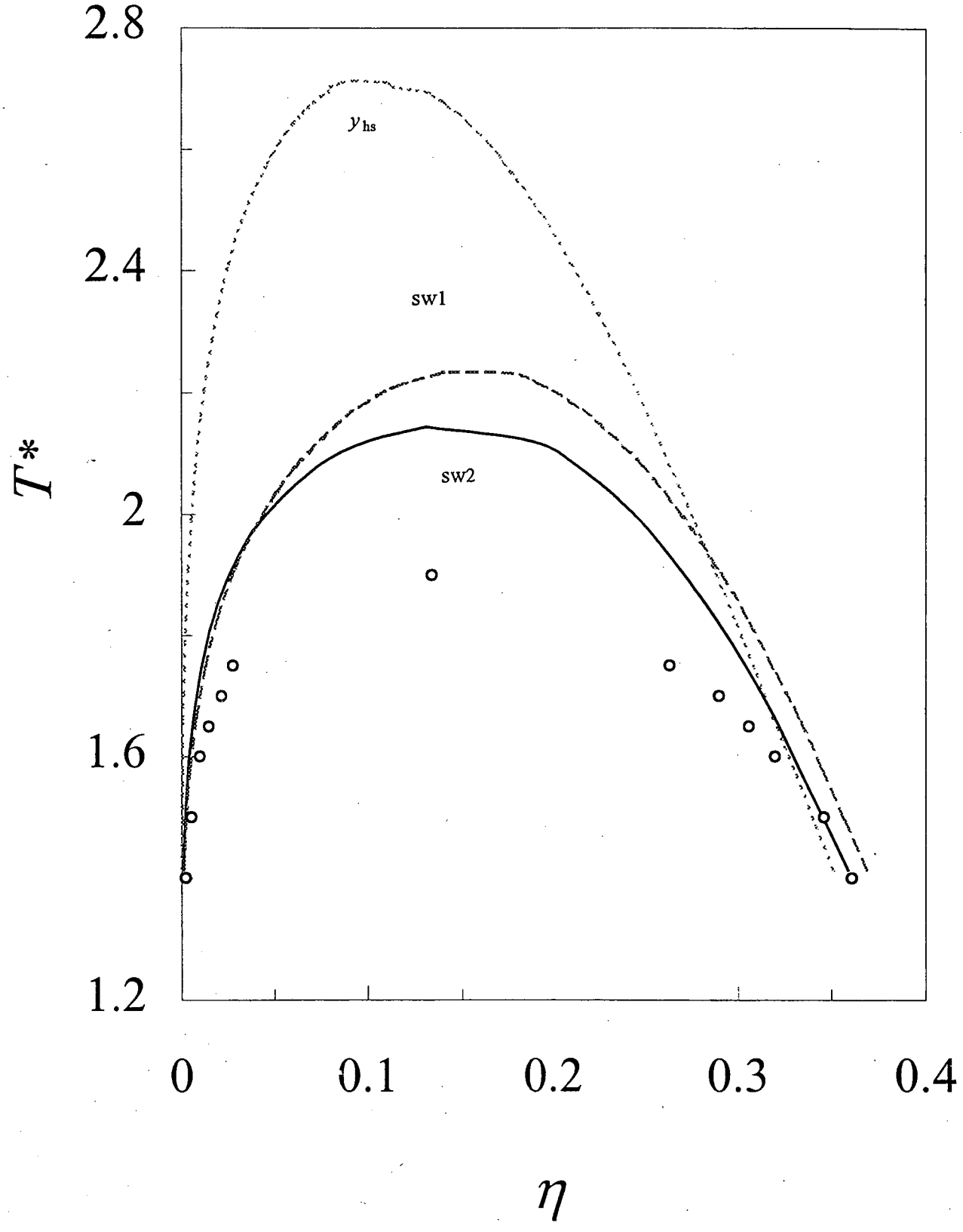

Fig.2

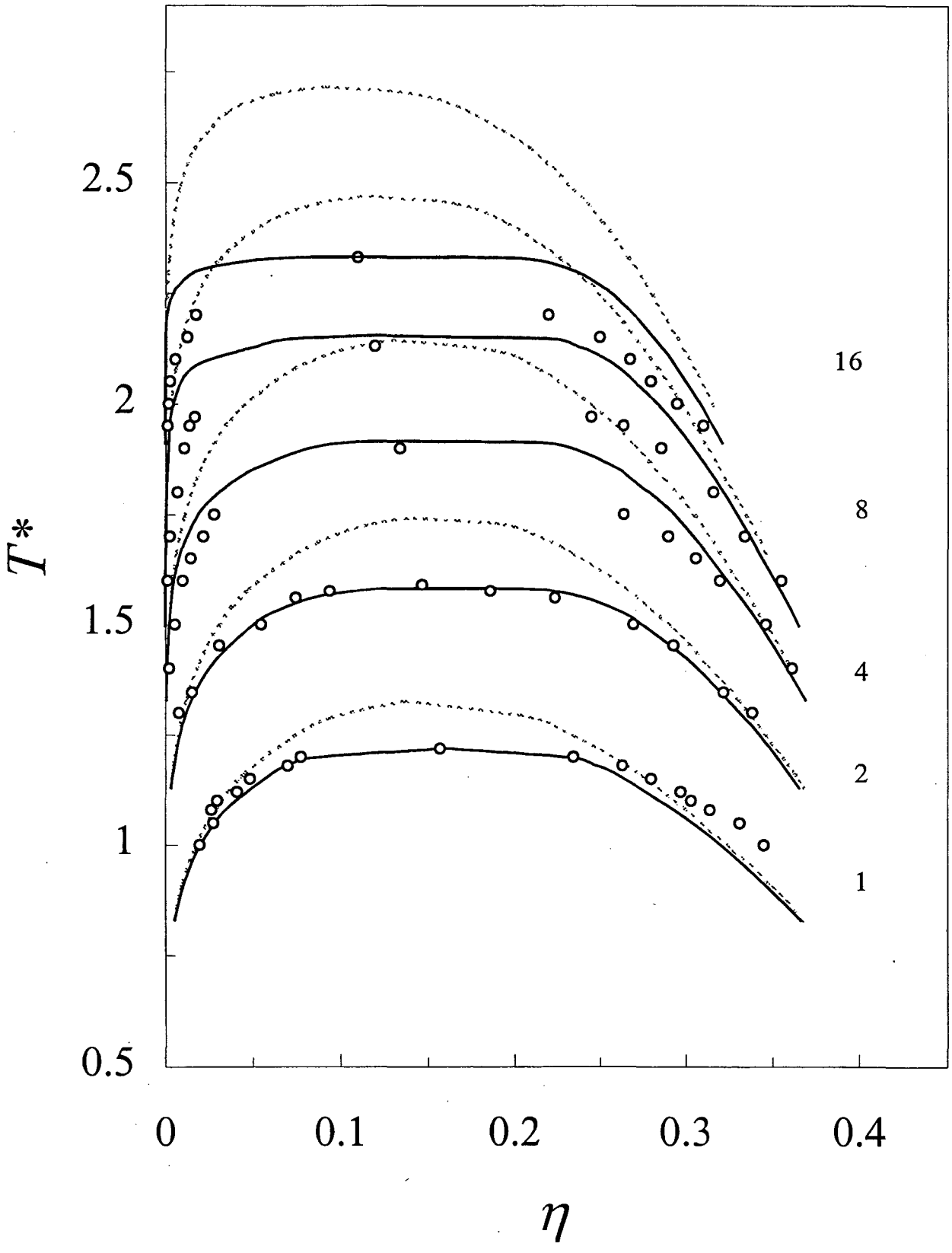

Fig.3

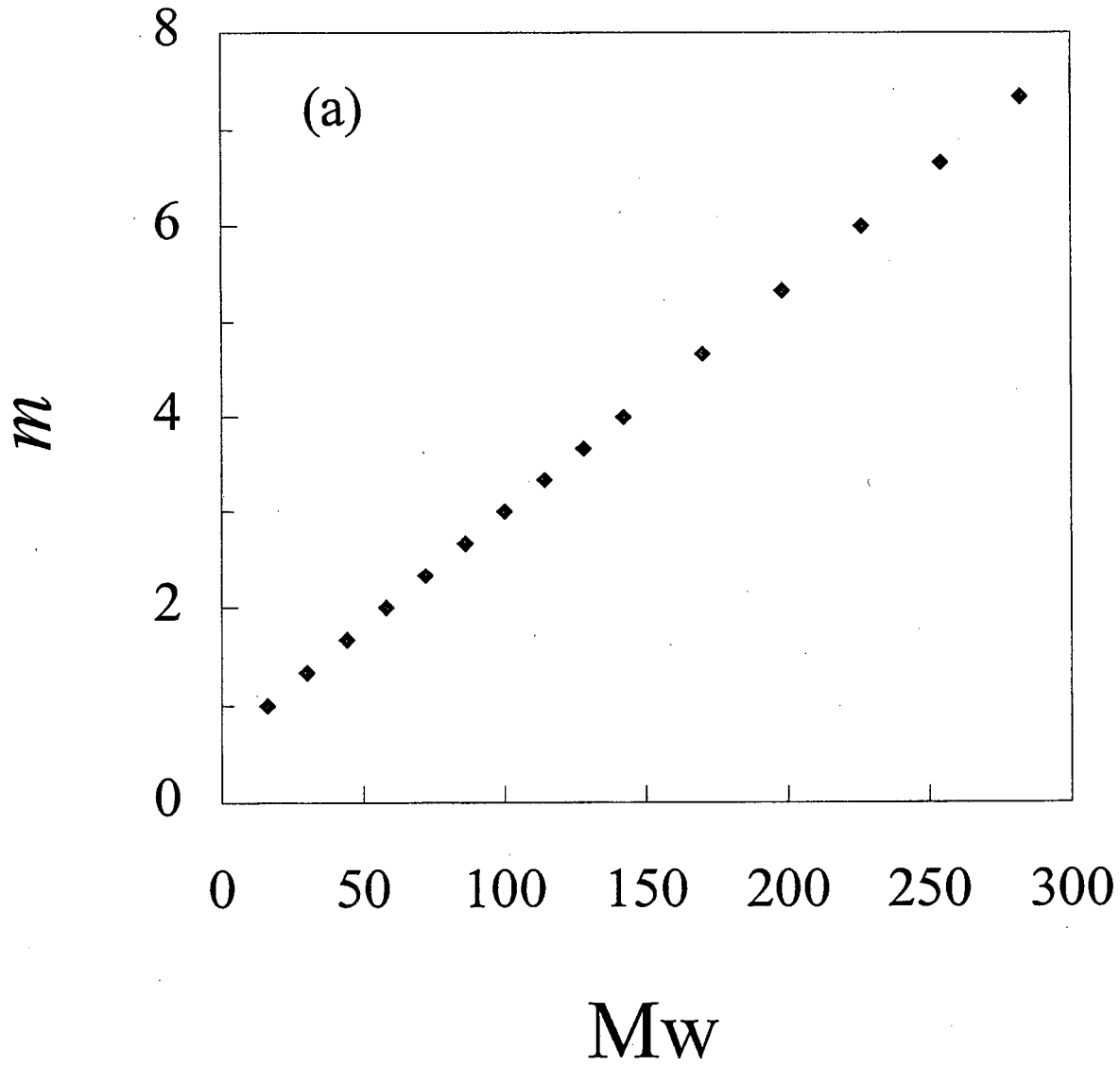

Fig.3

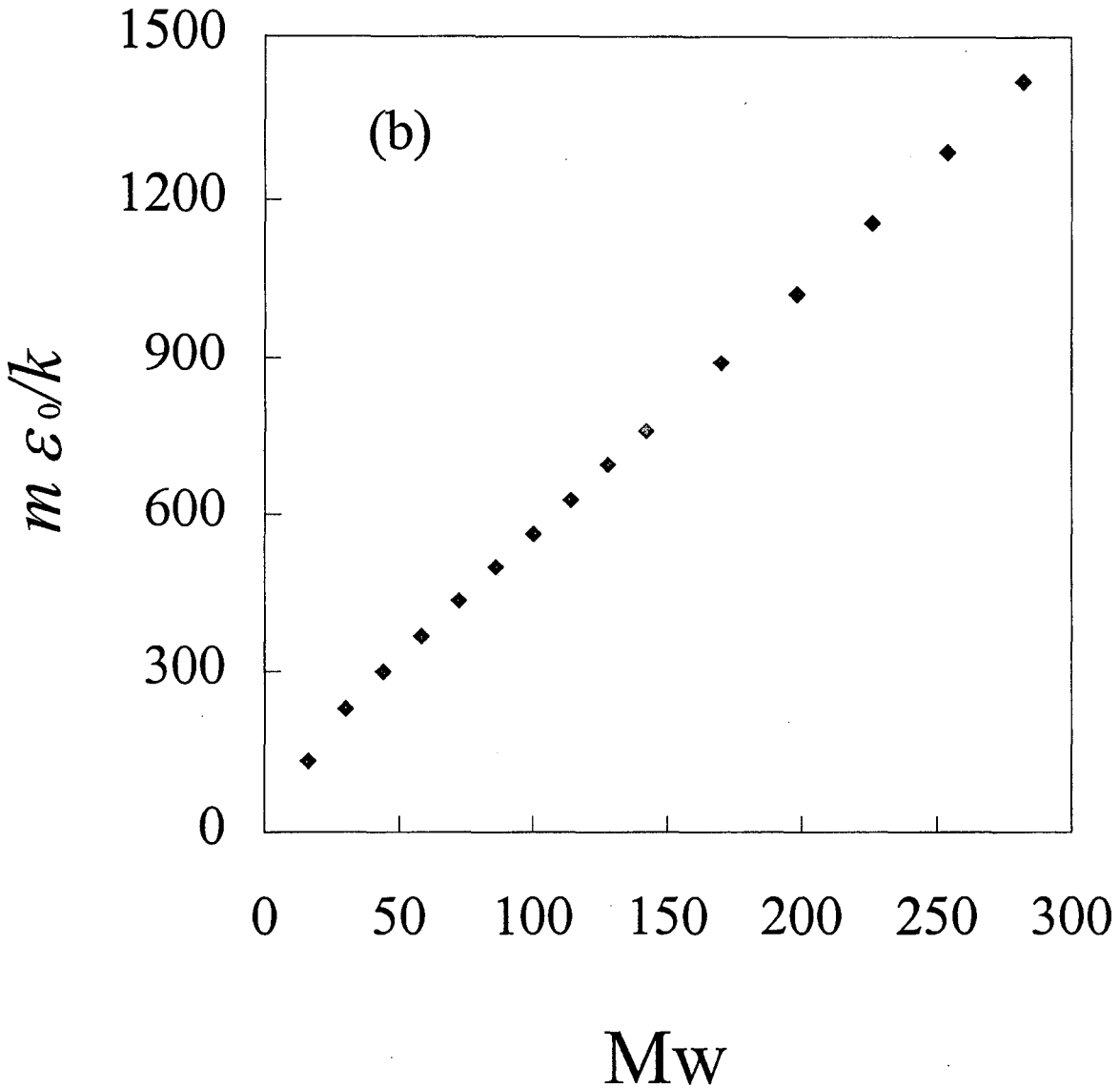
(b)
1500
1200
900
600
300
0
$m\,\varepsilon_0/k$
0
50
100
150
200
250
300
Mw

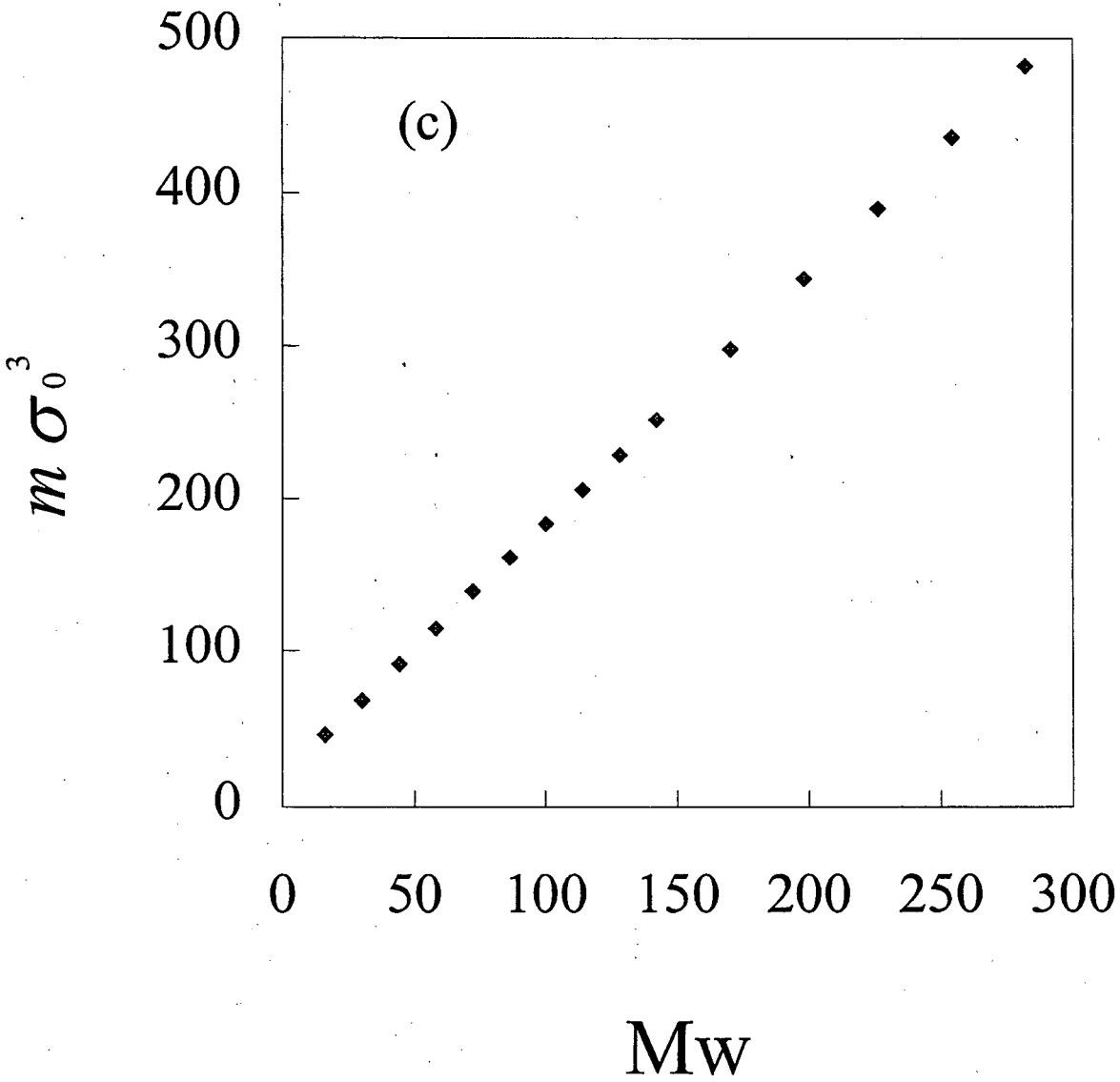
(c)
500
400
300
200
100
0
$m\,\sigma_0^3$
0
50
100
150
200
250
300
Mw

Fig.3

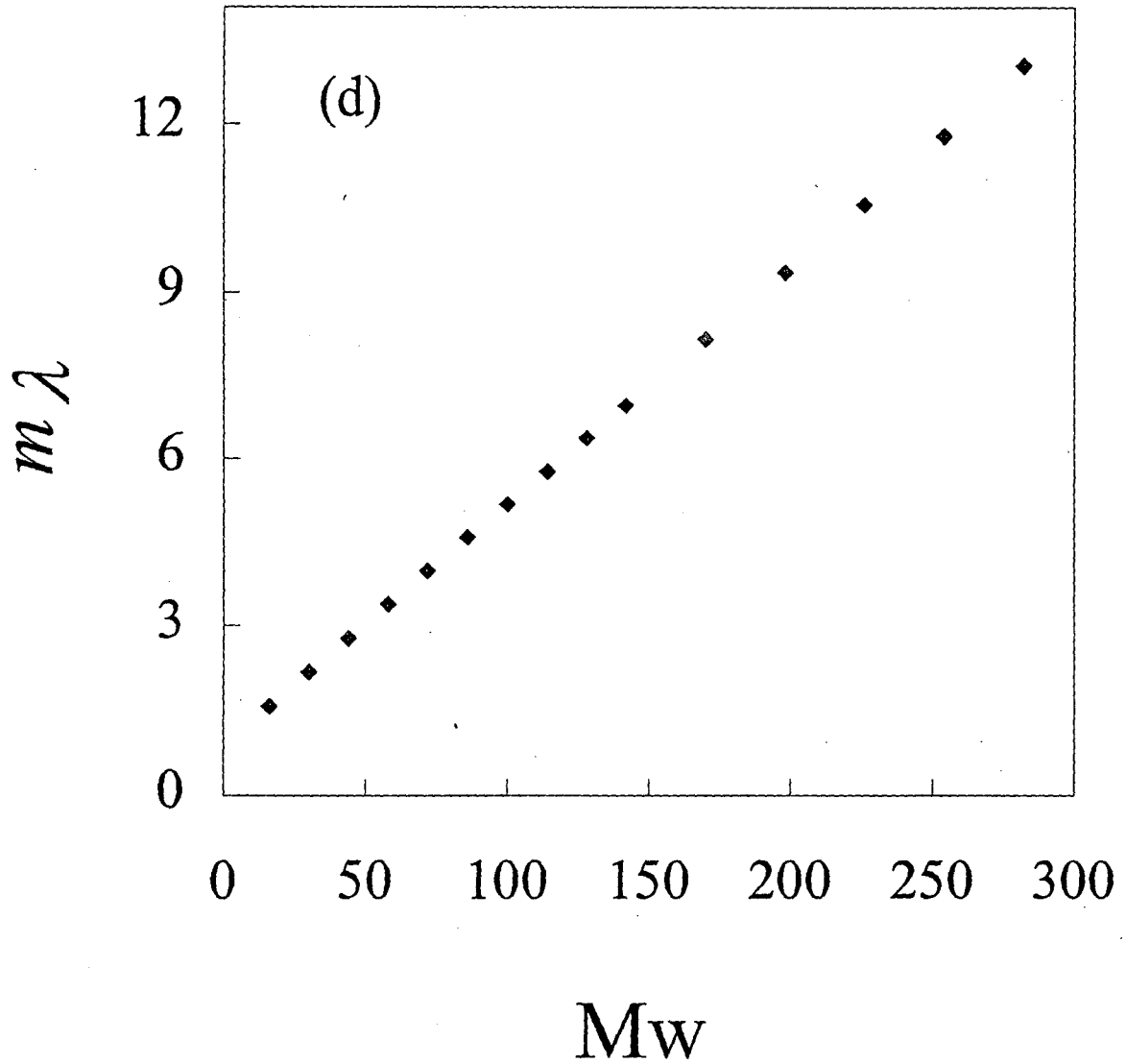

Fig.3

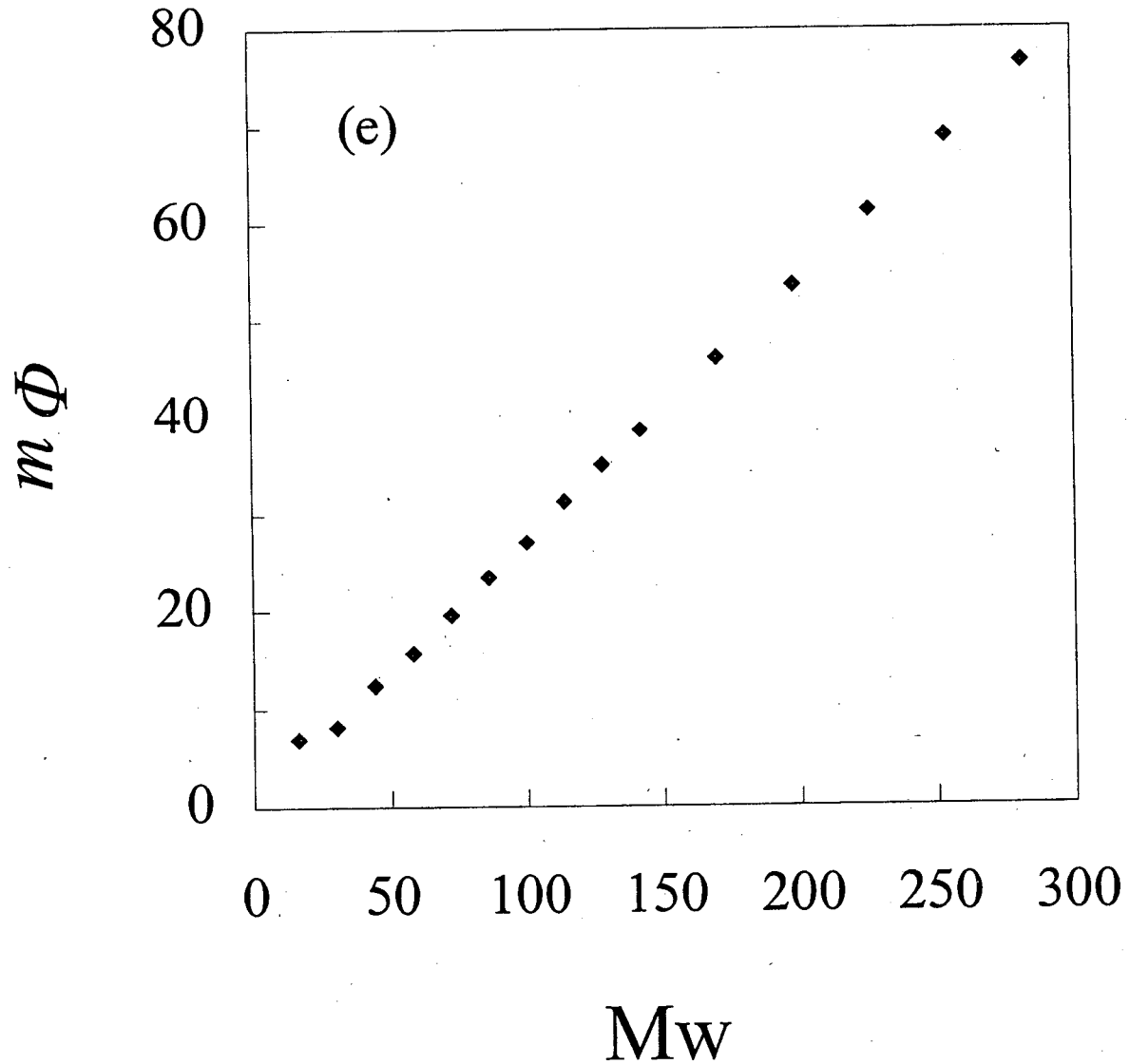

Fig.4

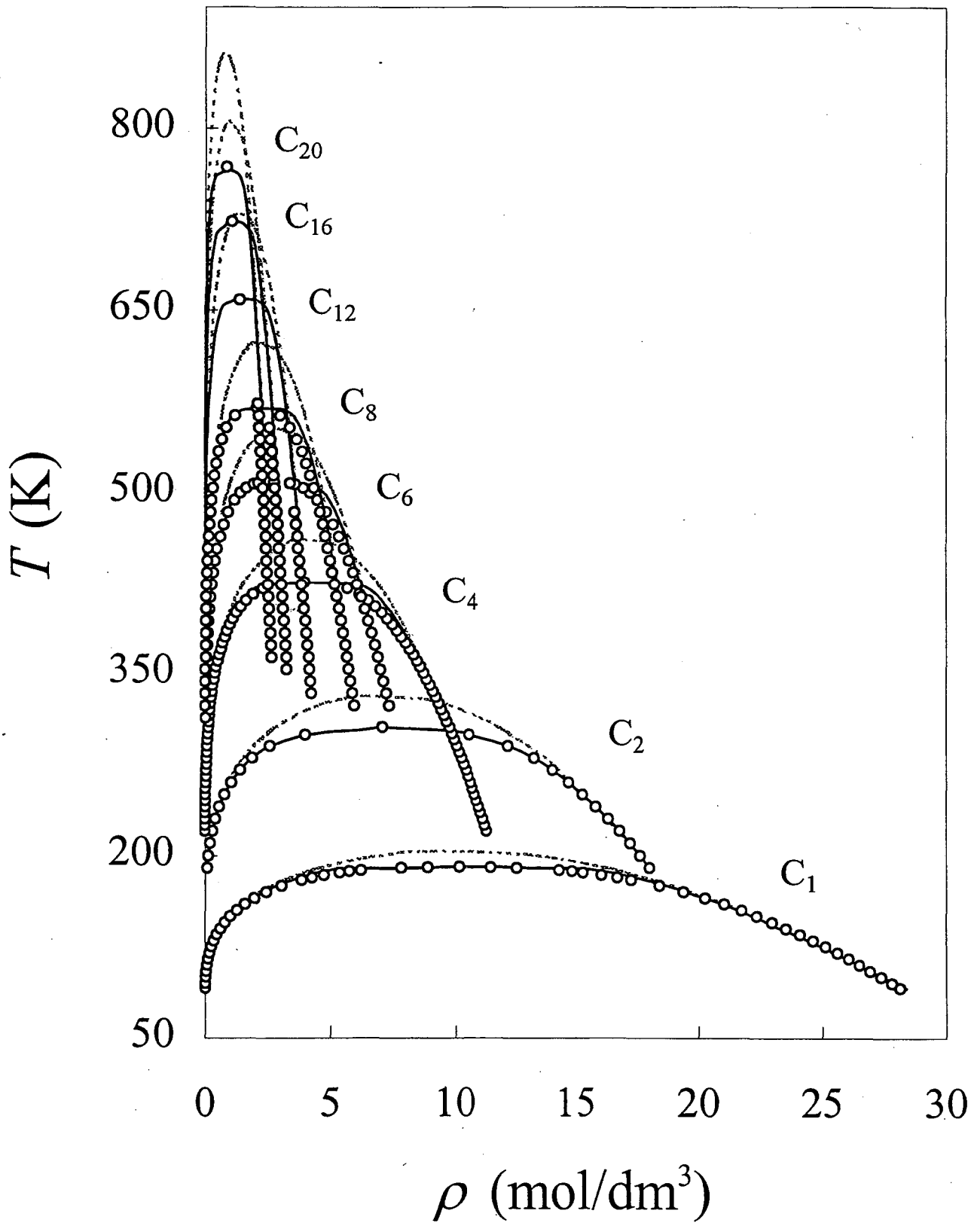
800
650
500
350
200
50
T (K)
C20
C16
C12
C8
C6
C4
C2
C1
0
5
10
15
20
25
30
ρ (mol/dm3)

Fig.5

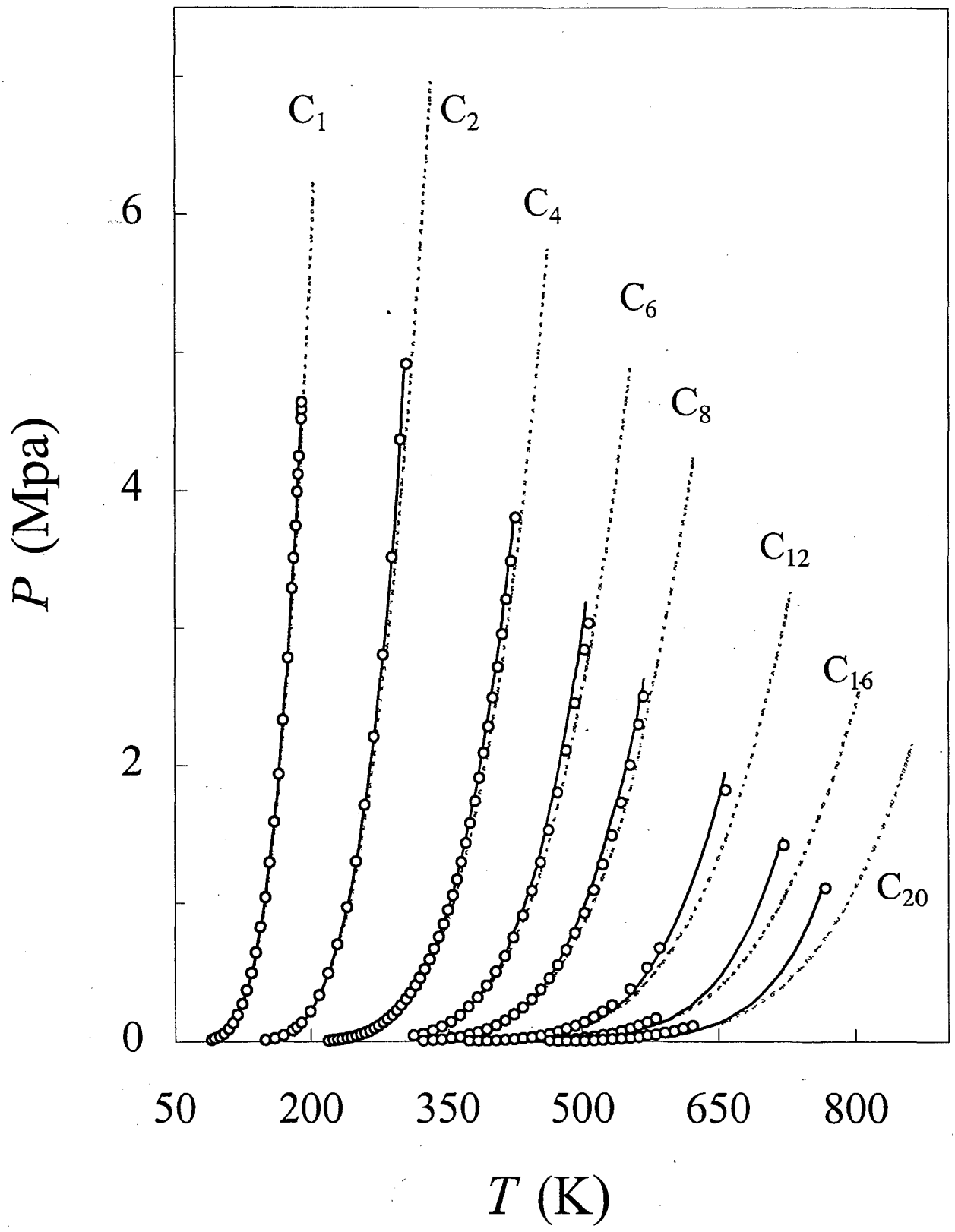

Fig.6

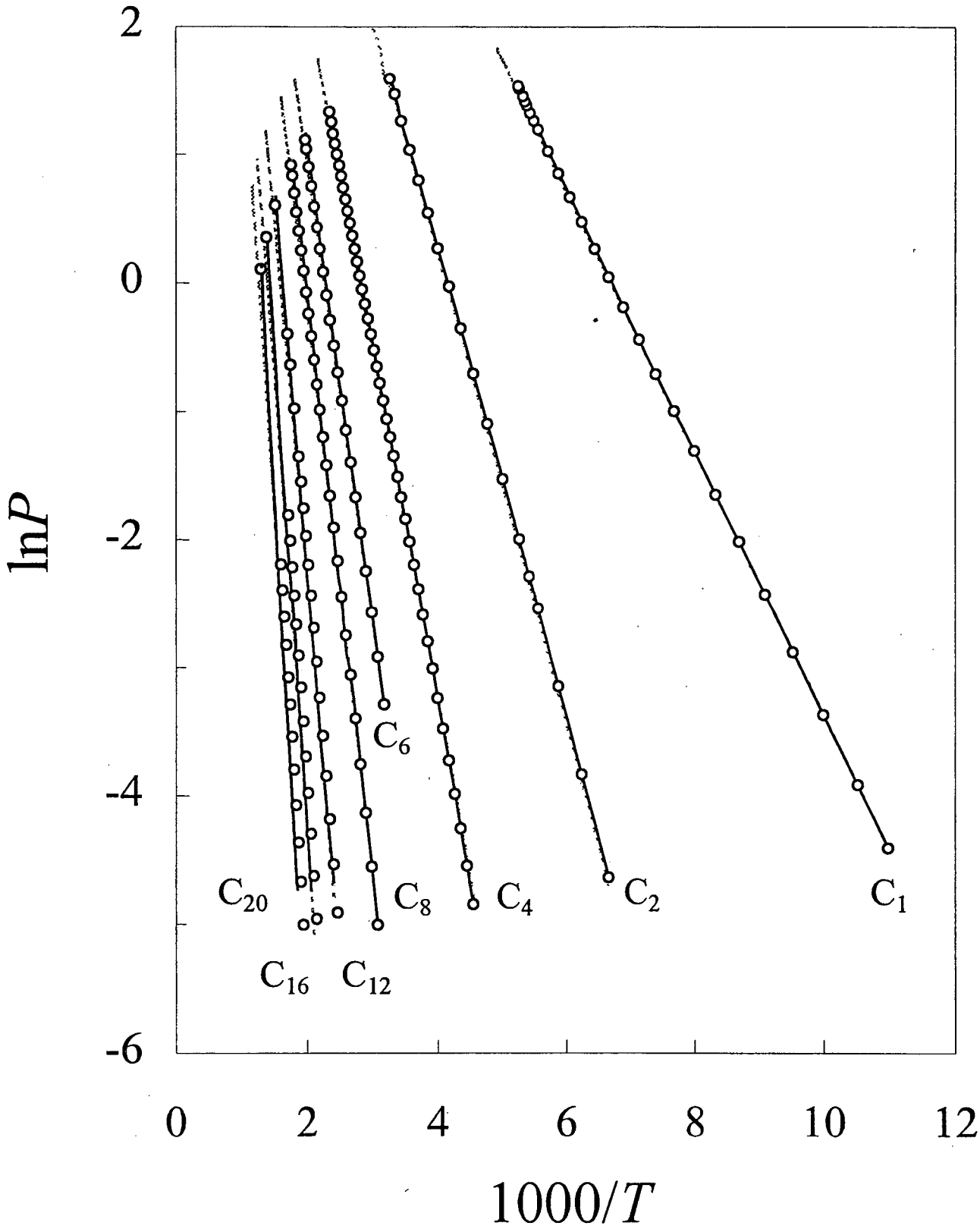

Fig.7

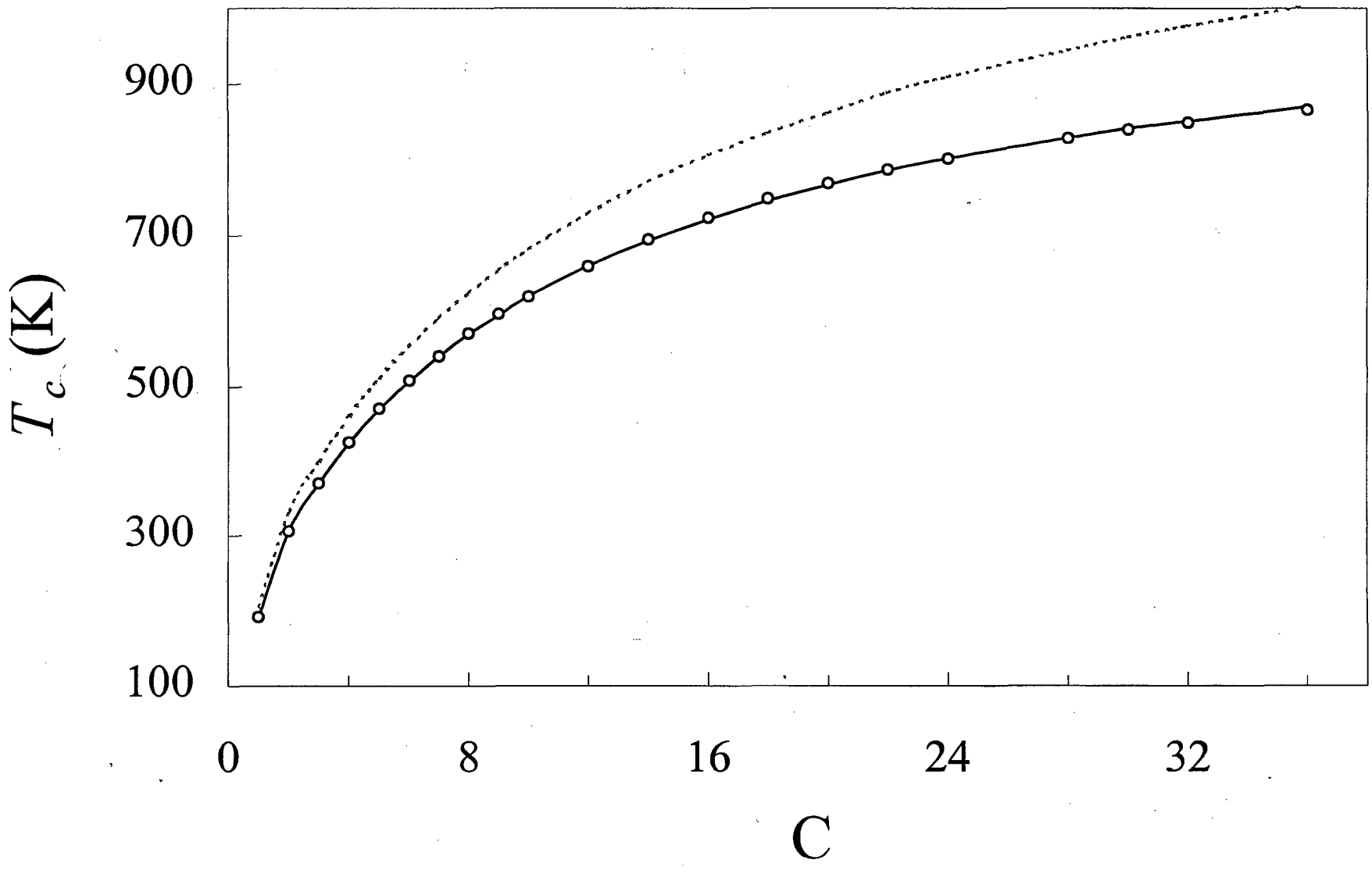

Fig.8

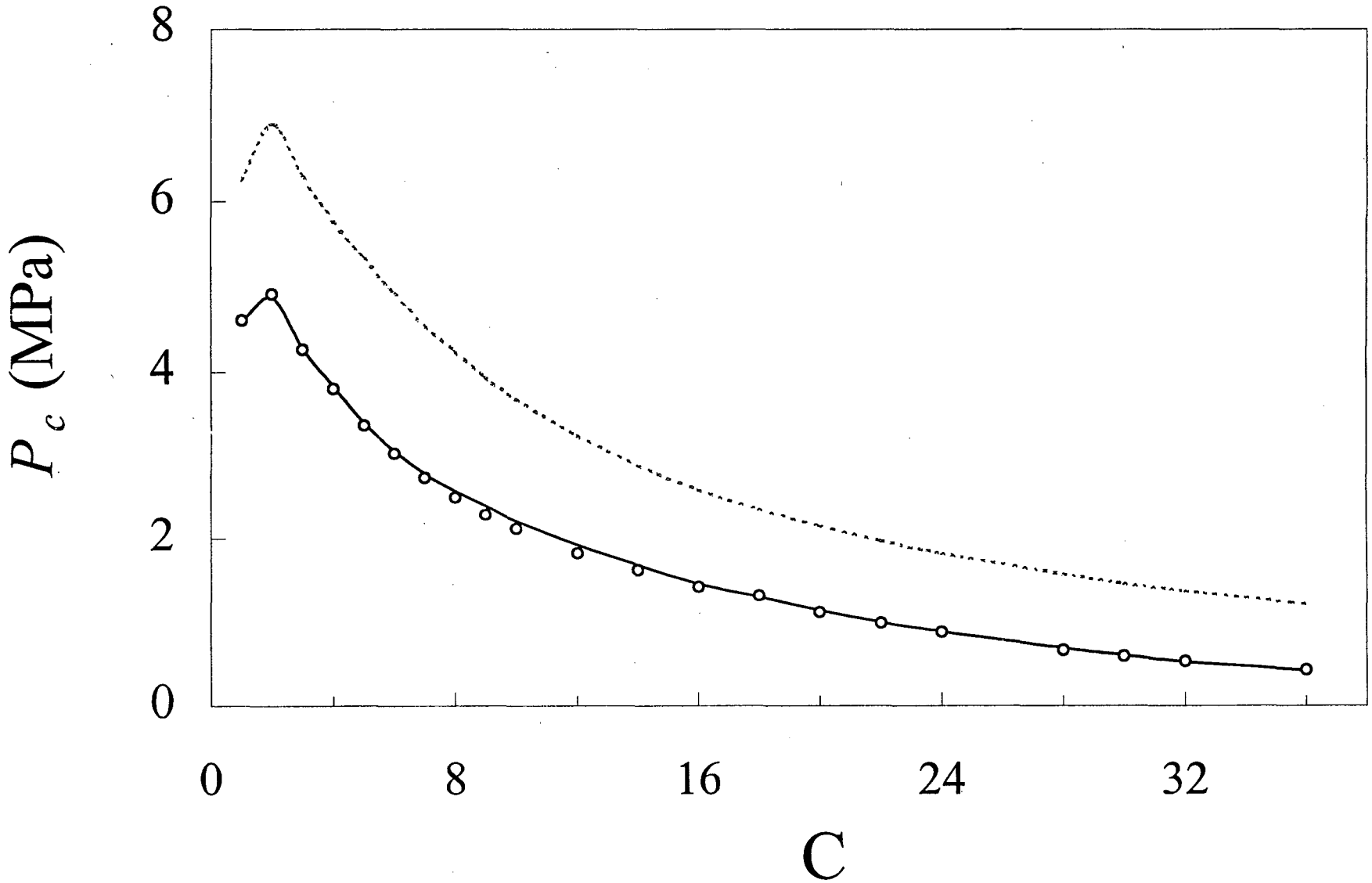

Fig.9

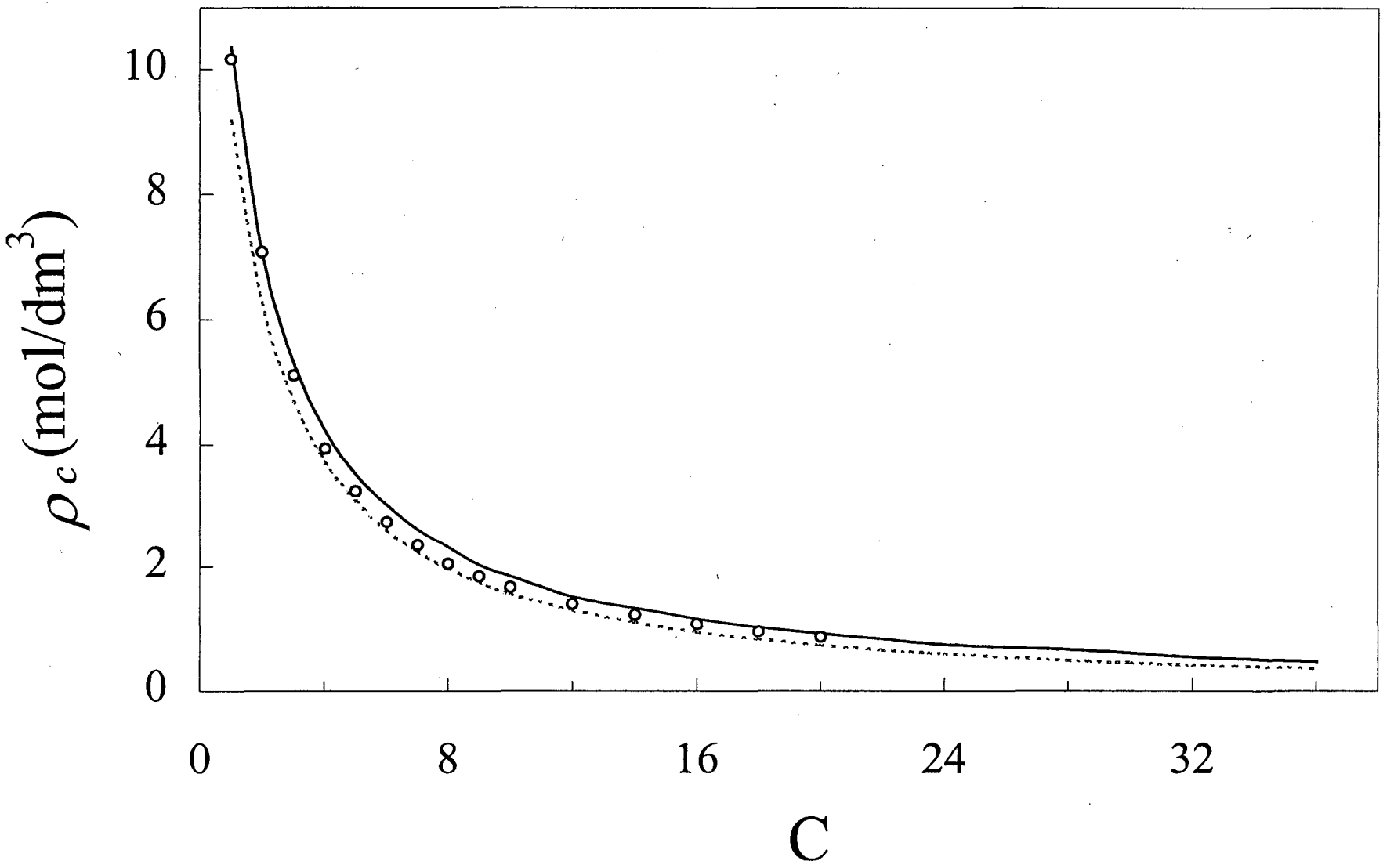

Fig.10

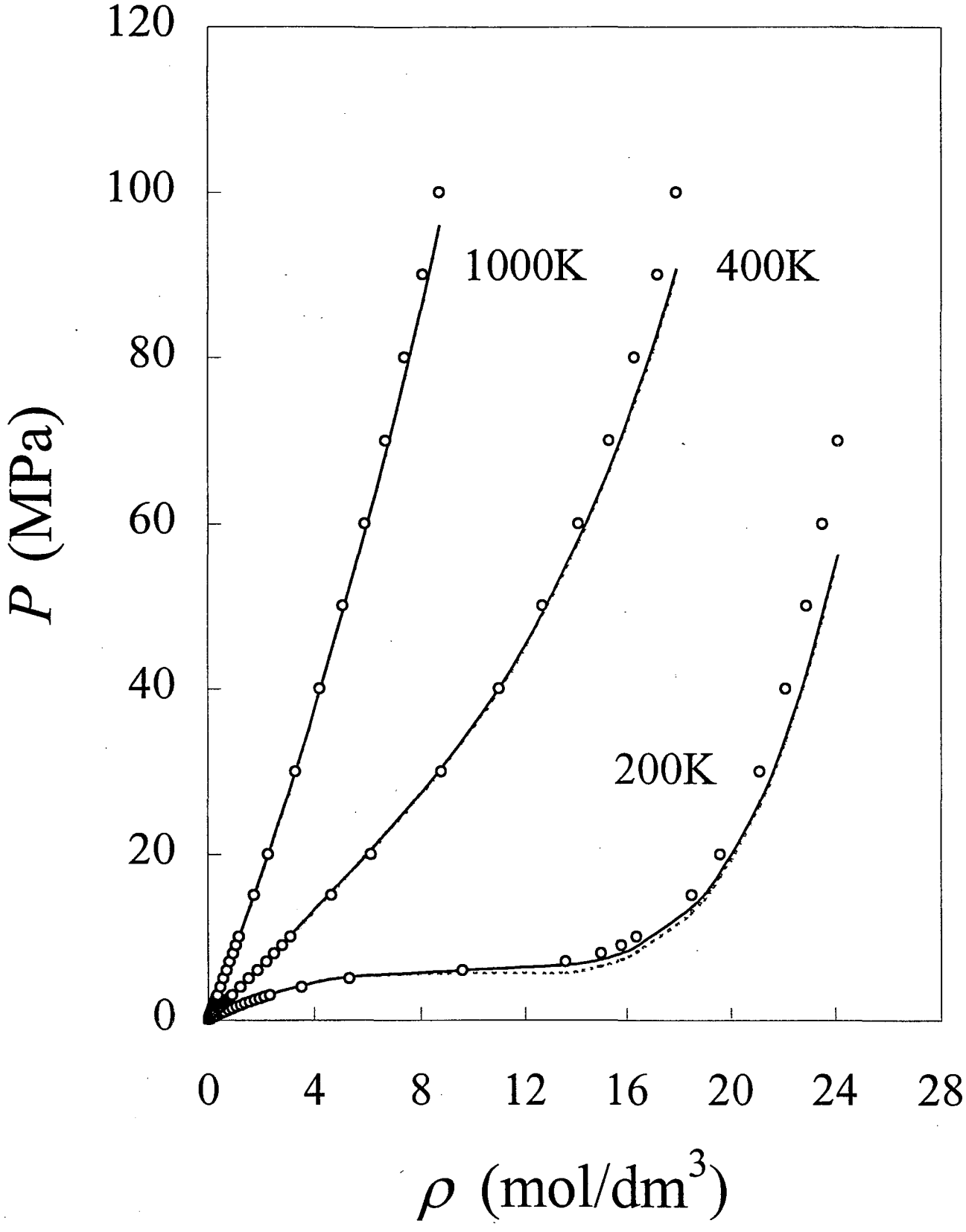
120
100
80
60
40
20
0
P (MPa)
1000K
400K
200K
0
4
8
12
16
20
24
28
ρ (mol/dm3)

Fig.11

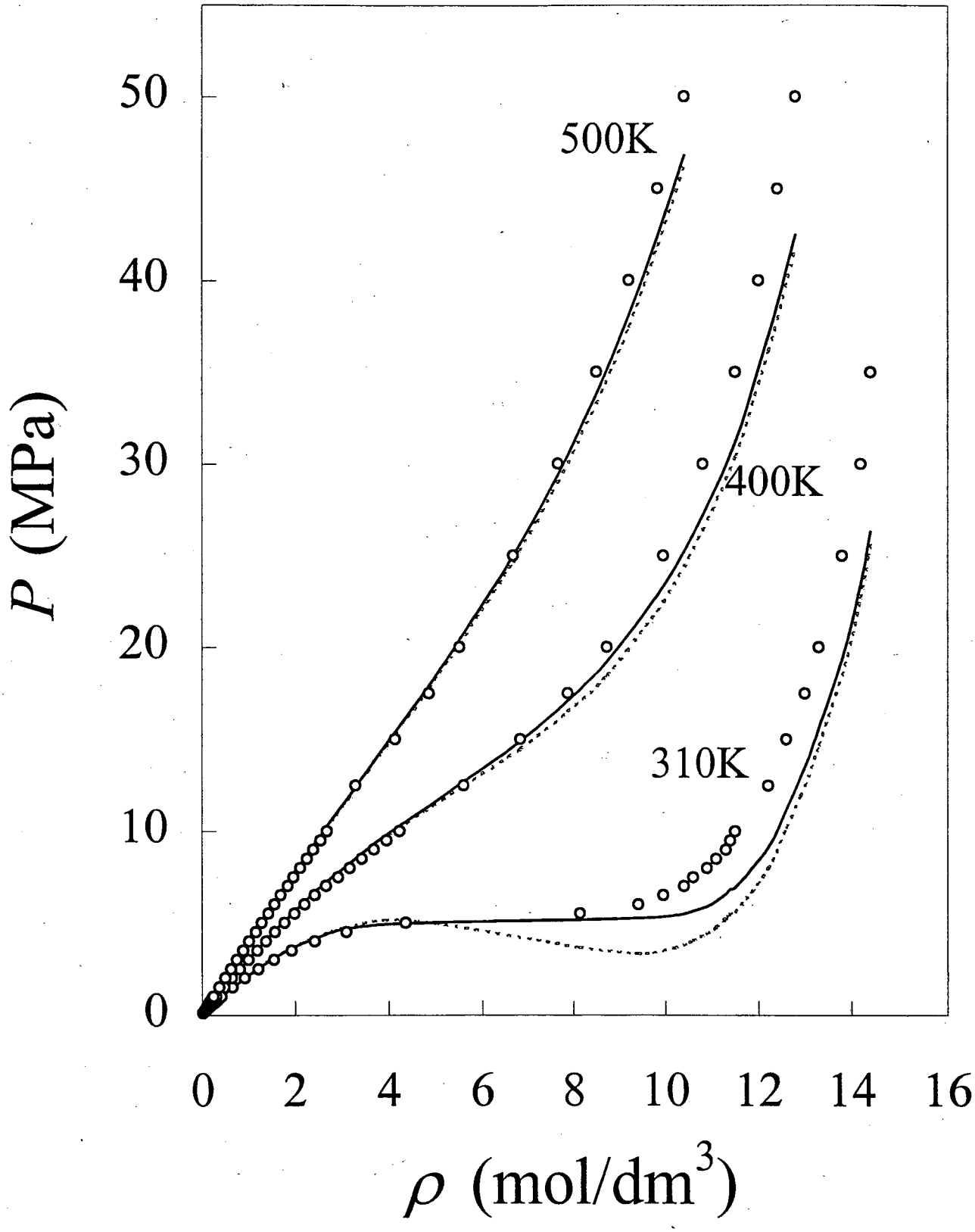

Fig.12

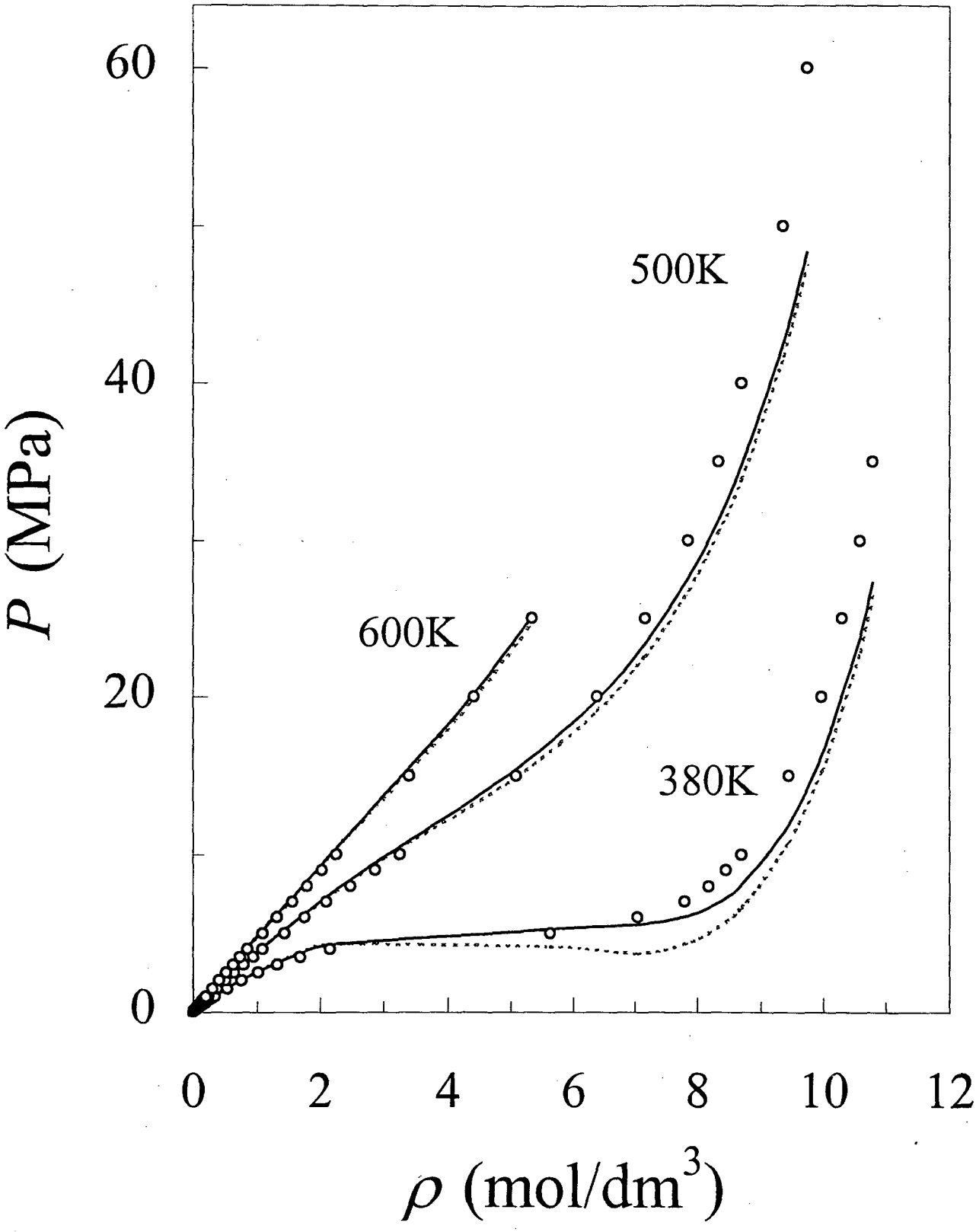

Fig.13

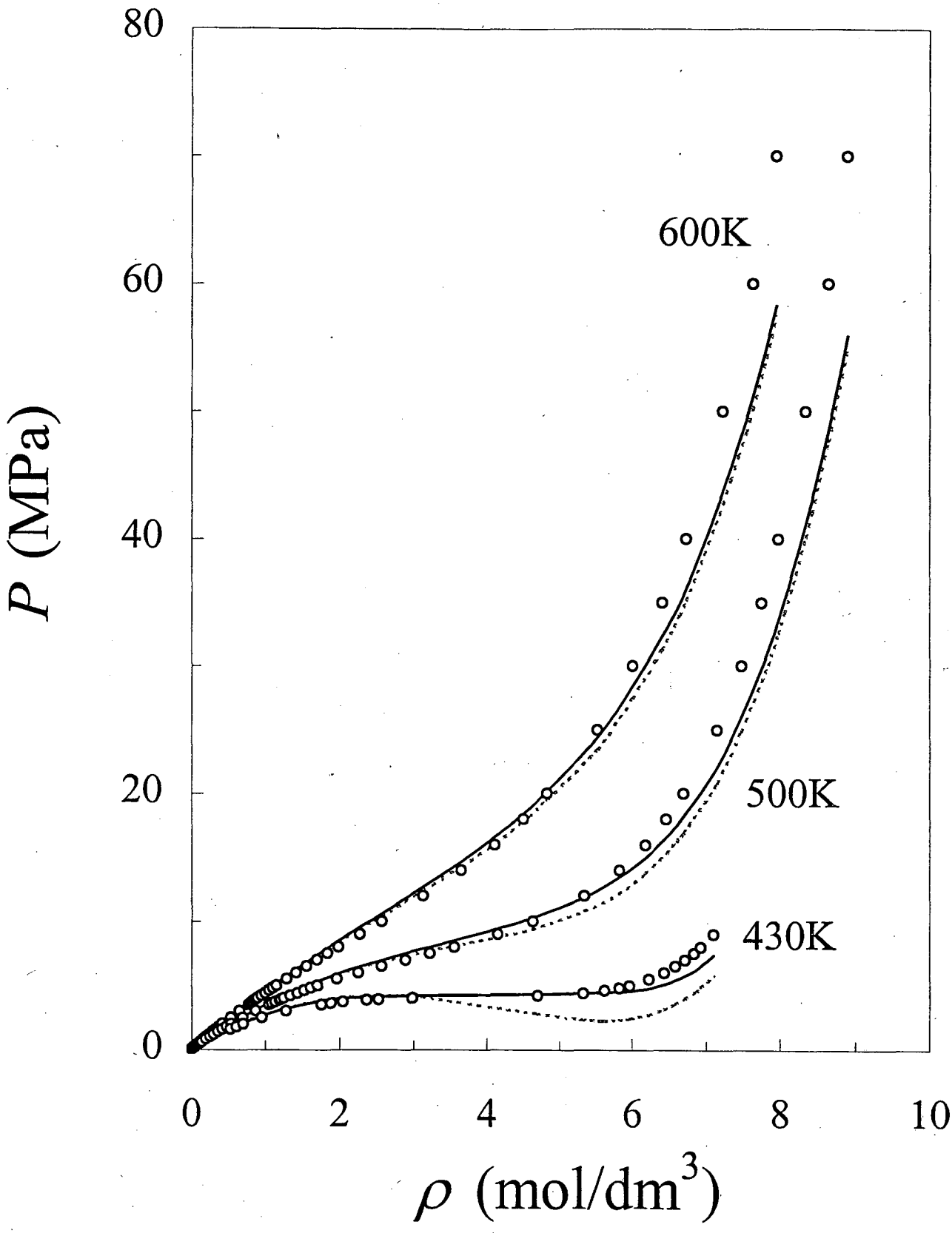

Ernest Orlando Lawrence Berkeley National Laboratory
One Cyclotron Road | Berkeley, California 94720

Prepared for the U.S. Department of Energy under Contract No. DE-AC03-76SF00098